Title:	Experimental verification of integral bridge abutments
Authors:	Muttoni A., Dumont A.-G., Burdet O., Savvilotidou M., Einpaul J., Nguyen M. L.
Published in:	Rapport OFROU
Pages:	86 p.
Country:	Switzerland
Year of publication:	2013
Type of publication:	Report

Please quote as:	Muttoni A., Dumont A.-G., Burdet O., Savvilotidou M., Einpaul J., Nguyen M. L., *Experimental verification of integral bridge abutments*, Rapport OFROU, Switzerland, 2013, 86 p..

Schweizerische Eidgenossenschaft
Confédération suisse
Confederazione Svizzera
Confederaziun svizra

Eidgenössisches Departement für Umwelt, Verkehr, Energie und Kommunikation UVEK
Département fédéral de l'environnement, des transports, de l'énergie et de la communication DETEC
Dipartimento federale dell'ambiente, dei trasporti, dell'energia e delle comunicazioni DATEC

Bundesamt für Strassen
Office fédéral des routes
Ufficio federale delle Strade

Experimental verification of integral bridge abutments

Vérification expérimentale des culées de ponts intégrés)

Experimentelle Überprüfung von Widerlagern integraler Brücken

École Polytechnique Fédérale de Lausanne (EPFL)
Laboratoire de construction en béton (IBETON)

Aurelio Muttoni, Prof.
André-Gilles Dumont, Prof.
Olivier Burdet, Dr.
Maria Savvilotidou
Jürgen Einpaul
Mai Lan Nguyen, Dr.

Mandat de recherche AGB 2009/015_OBF sur demande de L'Office Fédéral des Routes (OFROU)

Décembre 2013 **656**

Schweizerische Eidgenossenschaft
Confédération suisse
Confederazione Svizzera
Confederaziun svizra

Eidgenössisches Departement für Umwelt, Verkehr, Energie und Kommunikation UVEK
Département fédéral de l'environnement, des transports, de l'énergie et de la communication DETEC
Dipartimento federale dell'ambiente, dei trasporti, dell'energia e delle comunicazioni DATEC

Bundesamt für Strassen
Office fédéral des routes
Ufficio federale delle Strade

Experimental verification of integral bridge abutments

Vérification expérimentale des culées de ponts intégrés)

Experimentelle Überprüfung von Widerlagern integraler Brücken

École Polytechnique Fédérale de Lausanne (EPFL)
Laboratoire de construction en béton (IBETON)

Aurelio Muttoni, Prof.
André-Gilles Dumont, Prof.
Olivier Burdet, Dr.
Maria Savvilotidou
Jürgen Einpaul
Mai Lan Nguyen, Dr.

Mandat de recherche AGB 2009/015_OBF sur demande de L'Office Fédéral des Routes (OFROU)

Décembre 2013 **656**

Impressum

Service de recherche et équipe de projet

Direction du projet
Prof. A.Muttoni

Membres
Prof. A.-G. Dumont
Dr O. Burdet
Dr M.L. Nguyen
Dr N. Bueche
J. Einpaul

Commission de suivi

Président
Dr Armand Fürst
Membres
Heinrich Figi
Dr Dario Somaini
Dr Manuel Alvarez
Dr Hans Rudolf Ganz

Auteur de la demande

Groupe de travail et de recherche en matière de ponts (AGB)

Source

Le présent document est téléchargeable gratuitement sur http://www.mobilityplatform.ch.

Table of contents

Summary

Integral and semi-integral bridges require less maintenance than standard bridges equipped with expansion joints and mechanical bearings. Consequently, an increasing number of integral or semi-integral bridges have been built over the past decades. The movements of the bridge ends caused by creep, shrinkage and temperature effects are approximately proportional to the length of the bridge and may become large in the case of longer bridges. They are directly transmitted, together with the earth pressure of the embankment, to the abutment and to the transition slab.

The transition slab transfers the displacements of the bridge to the road infrastructure. The results of the research “AGB 2005/018 Ponts à culée intégrée” [DREIER 2010] have shown that, for integral bridges, the deformations of the pavement in the vicinity of the abutment can remain acceptable for bridge lengths larger than the current limit of 100 - 150 m [OFROU 2011]. The aim of the current research project was to experimentally investigate the behaviour of a semi-integral bridge abutment to verify the results of research AGB 2005/018. Three tests were performed on a large scale model to investigate the effect of the geometry of the transition slab and the movement sequence on the behaviour of the pavement surface.

Displacements were imposed at the bridge end of the transition slab by pushing or pulling it with hydraulic jacks. The displacements of the pavement over the transition slab and further away was monitored. The experimental results show that several factors, such the buried depth at the end of the transition slab, the roughness of its top and bottom surfaces and the interaction between the soil and the back wall play significant roles in the behaviour. It was also shown that the material properties of the asphalt in the vicinity of the bridge end are critical to avoid premature cracking of the pavement.

Résumé

Les ponts intégrés et semi-intégrés demandent moins de maintenance que les ponts classiques avec joints de dilatation et appuis mécaniques. C'est pourquoi leur proportion est en augmentation croissante ces dernières décennies. Les mouvements aux extrémités des ponts, causés par le fluage, le retrait et les effets thermiques sont sensiblement proportionnels à la longueur du pont et peuvent devenir importants dans le cas d'un pont d'une certaine longueur. Ensemble avec la pression du remblai, ils sont directement transmis à la culée et à la dalle de transition.

La dalle de transition transmet les déplacements du pont à l'infrastructure routière. Les résultats de la recherche "AGB 2005/018 Ponts à culée intégrée" [DREIER 2010] ont montré que, pour les ponts intégrés, les déformations du revêtement au voisinage de la culée peuvent rester acceptables pour des ponts d'une longueur supérieure à la limite actuelle de 100 à 150 m [OFROU 2011]. Le but de la présente recherche était d'étudier expérimentalement le comportement d'une culée de pont semi-intégré afin de vérifier les résultats de la recherche AGB 2005/018. Trois essais ont été effectués sur un modèle à grande échelle pour étudier l'effet de la géométrie de la dalle de transition et de la séquence de déplacements sur le comportement du revêtement.

Les déplacements ont été imposes à l'extrémité côté pont de la dalle de transition en la poussant ou la tirant avec des vérins hydrauliques. Les déplacements du revêtement au-dessus de la dalle de transition et à une plus grande distance étaient suivis. Les résultats expérimentaux montrent que plusieurs facteurs, comme l'enfouissement à l'extrémité de la dalle de transition, la rugosité de ses surfaces supérieure et inférieure et l'interaction entre le sol et le mur de culée jouent un rôle important dans le comportement. Il a également été observé que les propriétés de l'asphalte au voisinage de l'extrémité du pont sont très importantes pour éviter une fissuration prématurée du revêtement.

Zusammenfassung

Integrale und semi-integrale Brücken weisen gegenüber Brücken mit mechanischen Auflagern und Fahrbahnübergängen eine Erleichterung im Unterhalt auf. Daher wurde diese Bauweise in den vergangenen Jahrzehnten immer häufiger eingesetzt. Die Verschiebungen der Brückenenden infolge Kriechen, Schwinden und Temperatureinwirkungen sind etwa proportional zur Brückenlänge und können bei langen Brücken grosse Werte erreichen. Derartige Verformungen werden, zusammen mit dem Erddruck der Hinterfüllung, bei semi-integralen und integralen Brücken direkt ins Widerlager und die Schleppplatte eingeleitet.

Die Schleppplatte leitet die aufgezwungenen Verschiebungen an den Strassenoberbau weiter. Die Ergebnisse des Forschungsprojektes „AGB 2005/018 Ponts à culée intégrée“ zeigen deutlich, dass die Verformungen des Fahrbahnbelages in der Nähe des Widerlagers integraler Brücken in einer akzeptablen Grössenordnung liegen. Dies gilt selbst für Brücken länger als 100 - 150 m, welche als aktuelle Maximallänge integraler Brücken angesehen werden [OFROU 2011]. In der vorliegenden Forschungsarbeit wurde das Verhalten von Widerlagern semi-integraler Brücken experimentell untersucht, mit dem Zweck, die Resultate des Forschungsprojekts AGB 2005/018 zu validieren. Der Einfluss der Schleppplattengeometrie und der Belastungsgeschichte auf das Verhalten des Fahrbahnbelags wurde an drei grossmassstäblichen Versuchskörpern untersucht.

Mittels hydraulischer Pressen wurden der Schleppplatte auf der Seite der Brücke zyklische Verschiebung auf Zug und Druck aufgezwungen. Dabei wurden die Verformungen des Fahrbahnbelages oberhalb der Schleppplatte und in einiger Distanz aufgenommen. Die Versuchsresultate zeigen, dass mehrere Faktoren wie z.B. die Schleppplattentiefe, die Oberflächenrauhigkeit der Plattenober- und unterseite oder die Boden-Bauwerk-Interaktion der Auflagerwand das Verhalten massgeblich beeinflussen. Zusätzlich konnte festgestellt werden, dass die Asphalteigenschaften des an das Auflager angrenzenden Fahrbahnbelages entscheidend sind, um eine vorzeitige Rissbildung im Belag zu verhindern.

1 Introduction

Over their service life, bridge decks contract and expand as a result of time-dependent and temperature effects. This results in longitudinal movements of the bridge superstructure at its moving end abutments. In standard bridges, the abutment is a separate construction which does not move. Mechanical devices are thus necessary to make these two parts compatible. This is usually achieved by introducing movable bearings to support the bridge and expansion joints at the level of the pavement (Figure 1(a)). These elements are known to be weak points of the bridge and to often require costly maintenance. This is why, for bridges with a moderate length, alternate solutions have been introduced in the form of semi-integral bridges that do not have expansion joints but have mechanical bearings and of integral bridges that have neither expansion joints nor bearings (figure 1(b)).

In practical applications, the maximum possible length of an integral bridge depends on the longitudinal strains acting on the bridge superstructure due to temperature and time-dependent effects. According to [OFROU 2011, Fig. 4.11], this length can reach 100 m for roads with a high traffic flow and 150 m for other roads ($u_{imp,adm}$ = 20 mm, resp. 30 mm). This length is significantly shorter for new concrete bridges, because of the effects of creep and shrinkage.

The use of innovative details can increase the maximum admissible displacement that can be transferred from the bridge superstructure to the ground without negative effects both on the structure and its use, and thus increase the maximum possible length for an integral bridge. The transition slab plays an important role in this context. In standard bridges, the function of the transition slab is to provide a smooth transition between the embankment and the bridge, even if some settlement occurs in the vicinity of the abutment due to lack of compaction (Figure 1 (a)). In integral bridges, it still fulfils this function but, because it is fixed to the movable end of the bridge, it also transfers longitudinal displacements into the ground (Figure 1 (b)).

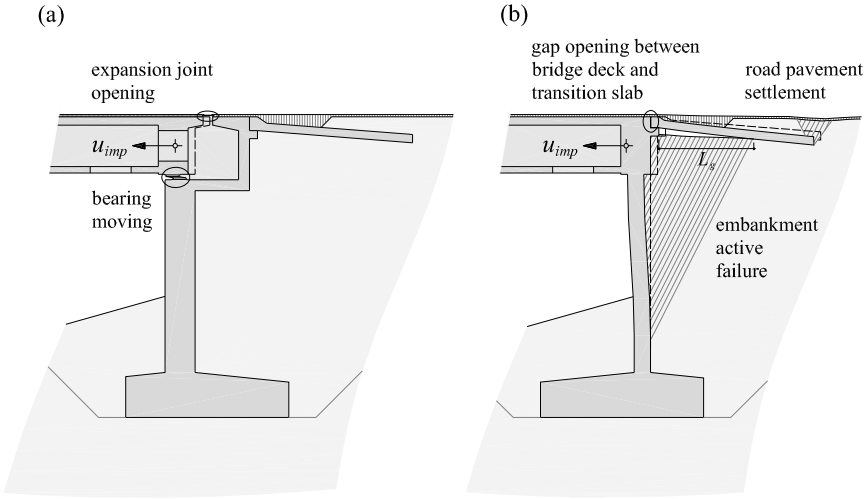

Figure 1: Potential problems caused by the longitudinal displacement of the bridge deck: (a) standard bridge; (b) integral bridge [DREIER 2010a]

In a previous FEDRO-supported research project, Dreier [DREIER 2010] highlighted three main problems that must be considered for the design of transition slabs of integral bridges as shown in Figure 1(b):

- When the bridge contracts, the abutment wall and the transition slab move together with the bridge superstructure and cause an active failure in the backfill behind the wall. This causes settlements at the surface over the length L_g. The length of the transition slab and its reinforcement must be designed so that the transition slab can effectively bridge over this zone.

- This movement also induces a rotation of the transition slab, which can propagate to the surface of the pavement and cause a gap to open. This can be solved by replacing the standard hinge of the solution shown in Figure 2 (a) [OFROU 2011] by a concrete hinge as shown experimentally in [DREIER 2009] (Figure 2(b)).

- Finally, the displacement imposed by the bridge deck causes a settlement of the pavement at the end of the transition slab. [DREIER 2010a, b] shows that increasing the depth at the end of the transition slab markedly reduces this effect. This can be achieved by increasing the inclination or the length of the transition slab.

(a)

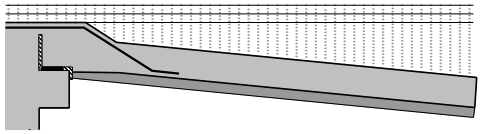

(b)

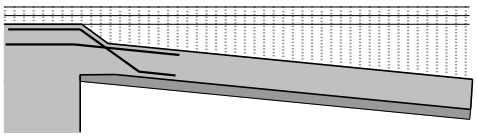

Figure 2: (a) Detail proposed by [OFROU 2011] and (b) improved connection detail between abutment and transition slab (for standard and integral abutments [DREIER 2011])

1.1 Previous research

The subject of soil-structures interaction in the vicinity of bridge ends of integral bridges has been the subject of several publications in the past decade. [White 2010] presents the results of a survey of the current practice on integral bridges in Europe. [Kaufmann 2005] and [Kaufmann 2009] present a state of the art review on integral bridges in Switzerland. [Kaufmann 2011] presents the current version of the Swiss directives on integral bridges.

[Kim 2010] and [Zhan 2013] discuss the effect of temperature changes on integral bridges.§ On site measurement results are presented in [Kerokoski 2006], [Pugasp 2009], [Petursson 2013] and in [Phares 2013]. [Zordan 2010] presents an analytical approach applicable to integral bridges.

IBETON conducted a previous research project on the subject of soil-structure interaction for integral bridges [DREIER 2010a]. The behaviour of the contact zone between the bridge end, the abutment, the transition slab, the soil and the pavement was investigated on the basis of numerical analyses to evaluate the settlement of the pavement caused by the longitudinal displacement of the bridge deck u_{imp}. The embankment was modelled using a Hujeux soil model while the concrete

structure was modelled as linear-elastic, with a reduced Young modulus for the transition slab to take into account its cracking. The behaviour of the asphalt layer was modelled as linear-elastic, with a very low modulus of elasticity instead of its actual viscous behaviour.

The main parameters of the embankment assumed in the model correspond to a well graded gravel backfill with a limited proportion of fines, as it typically used for highways. The geometry of the transition slab, shown in Figure 3 (a), corresponds to the Swiss recommendations for transition slabs of integral bridges [OFROU 2011], with a length L_{TS} = 6 m, an in inclination α_{TS} = 10%, a thickness h_{TS} = 0.3 m and an initial embedment depth $e_{TS,0}$ = 0.1 m. The numerical results indicate that the largest vertical displacements occur for imposed displacement in the active direction, when the bridge contracts. This action pulls the bridge end to the left, as shown in Figure 3 (a).

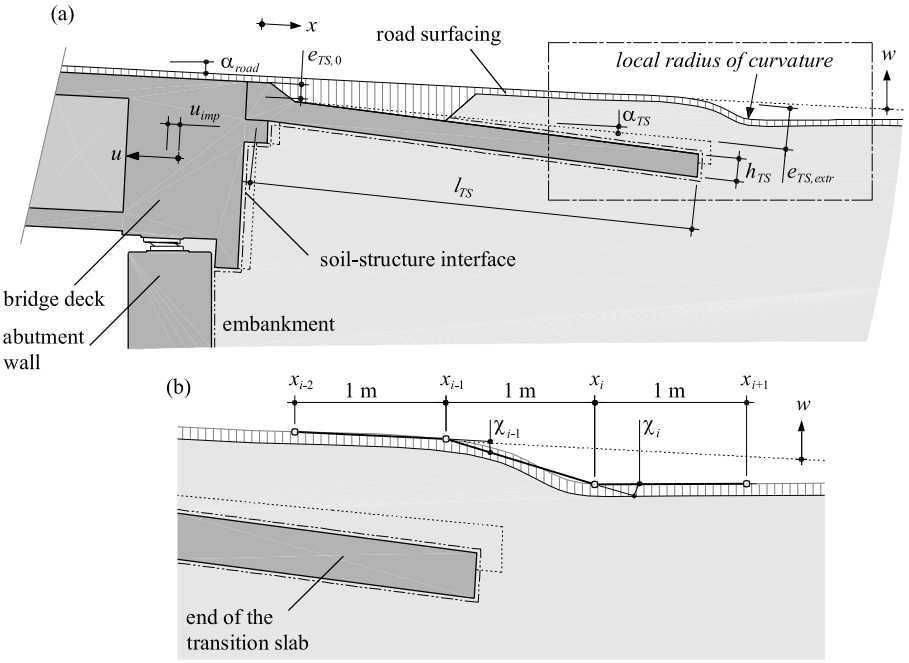

Figure 3: Numerical study
(a) geometry of a semi-integral bridge abutment ;
(b) geometric definition of the local curvature [DREIER 2011]

According to the VSS code [SN 640 520a], the serviceability limit state of the pavement at the end of the transition slab is governed the by the local curvature of the pavement surface. This parameter characterises the discomfort experimented by road users passing over a zone of settlement. The VSS code [SN 640 521c] defines the maximum value of the pavement curvature as χ_{adm} = 20‰ for highways over the service life of the pavement. This curvature was determined as shown in Figure 3(b), as a variation of slope over a length of one meter.

The curvature of the pavement χ, which depends on the imposed displacement u_{imp}, was determined on the basis of the surface deformations obtained from the numerical analysis. The maximum admissible horizontal displacement $u_{imp,adm}$ corresponds to the maximum curvature χ_{adm}. On the basis of $u_{imp,adm}$, the maximum distance between the fixed point and the abutment $L_{fp,adm}$, can be estimated using equation (1).

$$L_{fp,adm} = |u_{imp,adm} / \varepsilon_{imp}| \qquad (1)$$

where $\varepsilon_{imp} = \varepsilon_{\varphi} + \varepsilon_{sh} + \varepsilon_{\Delta T,min}$

The imposed strain ε_{imp} is the sum of the strain components due to concrete creep ε_{φ} and shrinkage ε_{sh} as well as the maximal negative temperature variations $\varepsilon_{\Delta T,min}$ of the bridge deck. In [DREIER 2010], the following set of values was used: $\varepsilon_{imp} \approx$ - 0.8 mm/m with $\varepsilon_{\varphi} \approx$ -0.3 mm/m, $\varepsilon_{sh} \approx$ -0.3 mm/m and $\varepsilon_{\Delta T,min} \approx$ -0.2 mm/m.

For a standard geometry of the transition slab (L_{TS} = 6 m, α_{TS} = 10 %), the numerical results give an admissible displacement $u_{imp,adm.}$ = 43 mm. According to equation (1), the maximal distance between the abutment and the fixed point of the bridge is $L_{fp,adm}$ = 54 m. For an integral concrete bridge with a fixed point at its midpoint, the largest possible length is then 108 m.

An interesting possibility is to transform an existing standard bridge into a bridge with integral or semi-integral abutments at the time of a major retrofitting (Figure 4). For concrete bridges, a large part of the time-dependent effects will have already happened, so that most of the remaining deformations to take into account are those related to thermal effects. Consequently, the maximum possible distance between the new integral abutments and the fixed point of the bridge can be significantly larger. The same calculation as above with $\varepsilon_{imp} \approx$ -0.4 mm/m ($\varepsilon_{\varphi} \approx$ -0.1 mm/m, $\varepsilon_{sh} \approx$ -0.1 mm/m and $\varepsilon_{\Delta T,min} \approx$ -0.2 mm/m) indicates that $L_{fp,adm}$ = 108 m. A similar calculation can be made for a steel bridge, which has no time-dependent effects but more severe temperature variations: with $\varepsilon_{imp} \approx$ -0.30 mm/m, $L_{fp,adm}$ = 143 m.

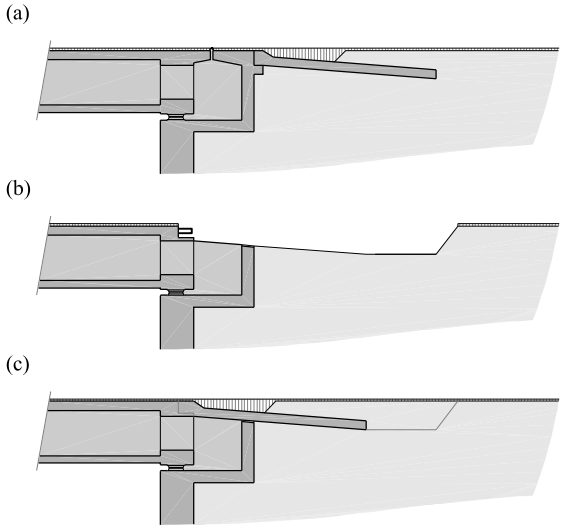

Figure 4: Transformation of an abutment with joints into a semi-integral abutment: (a) initial situation; (b) excavation of the embankment and removal of part of the existing bridge end; (c) reconstruction of the transition slab [DREIER 2010]

An imposed displacement in the passive direction, i.e. when the bridge expands, is less problematic. Taking only thermal effects into account, $\varepsilon_{imp} \approx$ 0.2 mm/m = $\varepsilon_{\Delta T,max}$ for a concrete bridge, the numerical results indicate that $u_{imp,adm}$ = -52 mm is acceptable for highways, which corresponds to a maximal length to the fixed point $L_{fp,adm}$ = 260 m.

A parametric study was performed to investigate the effect of a variation of the length of the transition slab L_{TS} and of its inclination α_{TS}. The thickness of the transition slab was kept constant h_{TS} = 0.3 m. Figure 5 shows clearly the strong influence of the buried depth at the end of the transition slab $e_{TS,extr}$ (Equation (2)). Starting at approximately 0.6 m, a strong increase of the admissible displacement is predicted for a moderate increase of the buried depth.

$$e_{TS,extr} = e_{TS,0} + L_{TS}\,\alpha_{TS} \qquad (2)$$

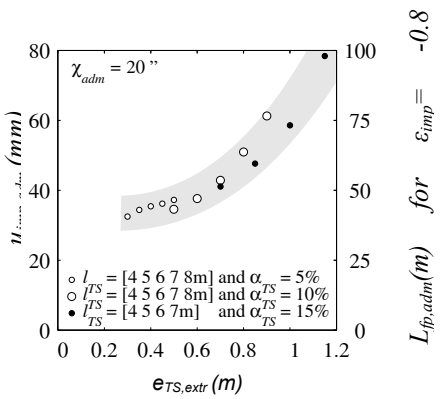

Figure 5: Parametric study: Influence of the buried depth at the end of the transition slab $e_{TS,extr}$ on the admissible imposed displacement $u_{imp,adm}$ [DREIER 2011]

As can be observed, the values of the maximum admissible imposed displacement $u_{imp,adm}$ of [DREIER 2011] exceed the current limit set by the Swiss Federal Roads Office (FEDRO) [OFROU 2011] *(u_{imp}* $\leq$ 20 mm for normal cases or $\leq$ 30 mm for exceptional cases).

The values presented in Figure 5 were derived from numerical simulations and need to be confirmed by experimental results. Potentially important effects such as cyclic effects in the soil and re-compaction of the soil by passing traffic were not included in the model. In particular, the possibility of pavement cracking caused by imposed deformations was not considered (pavement modelled as linear-elastic).

1.2 Objective of the research

The objective of the present research project was to investigate the validity of the theoretical results of the research presented in section 1.1. In the framework of this project, three tests were performed on a model of a semi-integral bridge abutment with a transition slab. The model included the back wall of the abutment and the inclined transition slab as well as the embankment, below and above the transition slab, and the pavement.

Hydraulic jacks were used to induce the horizontal displacements imposed by the bridge deck, both in pulling and in pushing. To simulate the effect of the passage of vehicles and the resulting compaction of the embankment, a pneumatic roller was used to compact the soil at the end of each movement phase.

The variables of the test series were:

- the inclination of the transition slab : 10 % as the most common value and 20 % to have a deeper buried depth at the end of the transition slab;
- the sequence of application of the displacements : tension first, compression first, cyclic loading;
- the surface condition of the transition slab: smooth surface at the top (as usual) or at the bottom.

The applied forces, the movements of the head of the transition slab, the ambient temperature and the temperature at the bottom of the asphalt layer were continuously monitored. The longitudinal and vertical displacements at the surface of the pavement were measured at the end of each movement phase.

The test setup was completed in September 2011. The first test took place from November 15 to 24, 2011 (4 effective testing days). The second test took place on December 6 and 7 and the third on February 22, 2012.

1.3 Organisation of the report

Chapter 2 describes the test setup, the testing procedure and the instrumentation.

Chapter 3 shows the results of the three tests and their interpretation.

Chapter 4 proposes practical considerations for the construction of transition slabs of integral bridges.

Chapter 5 contains proposals for the continuation of investigations on this topic.

Appendices A through F give details of the test setup and additional test results.

2 Test setup

2.1 Model of a semi-integral bridge abutment

To investigate the behaviour of the pavement in the vicinity of the transition slab, a large scale model of a semi-integral bridge abutment was constructed in a custom-built test environment on the campus of EPFL. Figure 6 shows the construction phases of the test setup that included the prefabricated lateral walls, the soil underneath and above the transition slab, the lean concrete and the transition slab, the back wall of the abutment and the pavement. To reduce the friction between the lateral walls and the embankment soil, layers of polystyrene (Sagex) covered by plastic sheets were placed along the side walls.

Figure 6: Construction of the test setup and positioning of the transition slab

(a) Placing of the prefabricated side walls; (b) test setup with lean concrete ready to receive the transition slab, notice the polystyrene plates and the plastic sheets on the side walls; (c) transition slab in place; (d) placement of the embankment above the transition slab; (e) transition slab with layer of bituminous paper ready to re-

ceive the asphalt layer in the vicinity of the slab head, notice the fibre cement plate on the side to limit lateral friction; (f) finished asphalt layer.

A prefabricated concrete beam served as a reaction element at the far end of the test setup, allowing its longitudinal post-tensioning by two Dywidag bars Ø 32 mm.

2.1.1 Transition slab

The transition slab has a symmetric geometry inspired from usual geometries for transition slabs (4.12 x 2.20 x 0.25 m, fig.8). It was prefabricated using C30/37 concrete with two different surfaces: a smooth and a rough face (Figure 7). Before each test, it was precisely positioned on a layer of lean concrete placed on the compacted backfill with the specified height and inclination.

Figure 7: Transition slab with its rough surface at the top

The transition slab was reinforced with 22 Ø 16/100 longitudinal steel bars and 30 Ø 14/150 transverse bars at the top and bottom faces. The slab head was reinforced with 22 Ø14/100 and 22 Ø 10/100 hairpin reinforcements. Appendix A shows the plan and details of the reinforcement of the slab. No cracking was observed at the surface of the transition slab after the first two tests.

2.1.2 Backfill and pavement structure

The backfill used for the foundation of the pavement was 1.50 m gravel II (new) 0/45. A layer of lean concrete was placed underneath the transition slab as would be in a real application.

The pavement layering consisted of:

- 0.35 m gravel I (unbound granular materials) 0/45
- 0.14 m bituminous asphalt: 0.09 m ACT22 S base layer and 0.05 m AC11 S final layer.

The pavement surface was approximately 9 m x 2.2 m. The quality, thickness and level of compaction of the backfill and pavement layers were chosen to be similar to those used for Swiss highways. The pavement used was not adapted to take into account possible large deformations induced by the bridge's movements, in particular due to temperature changes. This was done purposely, as the idea is that integral bridges should be "invisible" for the users and the maintenance crews alike. It could be advisable, however, to adopt a specifically formulated pavement solution with a high ratio of polymer modified bitumen, which can undergo larger elongations. Their suitability for the application to highways should be further checked (resistance to rutting in particular). Table 1 shows the characteristics of the structural pavement layer Type AC T 22 S (according to SN 640 431-21a-NA).

Table 1: Characteristics of the asphalt mix AC T 22 S used in the tests

Sieve size [mm]	Passing through (nominal) [%]
0.063	6.0
0.125	8.0
0.25	11.0
0.5	15.0
1.0	20.0
2.0	28.0
4.0	38.0
5.6	44.0
8.0	54.4
11.2	66.0
16.0	79.0
22.4	95.0
31.5	100.0
Binder contents (50/70 S)	4.3
Apparent volumic mass: 2.380 [t/m^3]	

2.1.3 Protecting tent and heating system

During the experiments, which took place in the winter time, the structure was covered by a tent. A fuel heating system by forced air was installed to maintain constant testing conditions.

2.2 Test Configurations

Three different tests were performed using the same transition slab in different configurations:

- Test TST1 was performed with the transition slab at a 20 % inclination with its rough surface on top. It was loaded monotonically, first in pulling, then in pushing.
- Test TST2 was performed with the transition slab at a 10 % inclination with its rough surface on top. It was loaded monotonically, first in pulling, then in pushing, and then was finally pulled back to its original position.
- Test TST3 was performed with the transition slab at a 20 % inclination with its smooth surface on top. It was loaded cyclically, first in compression, then in tension, for a total of three movement phases.

Table 2 summarizes the main parameters of the test series.

Table 2: Main parameters of the test series

	Positioning of the slab		Displacement sequence	Measurements									
	α_{TS} (%)	Surfaces top / bottom	(+ : pulling - : pushing)	Pavement			Slab Head			Walls		Temp.	
				u_{pav}	$u_{pav,edg}$	w_{pav}	u_{imp}	w_{TS}	$\Delta\alpha_{TS}$	u_{bw}	u_{rw}	T_{air}	$T_{pav,be}$
TST1	20	rough / smooth	Monotonic +/-	×	×	×	×		×	×	×	×	×
TST2	10	rough / smooth	Monotonic +/-/+	×	×	×	×		×	×	×	×	×
TST3	20	smooth / rough	Cyclic -/+		×	×	×	×	×	×		×	×

2.2.1 Position of the transition slab

Figures 8 to 10 show the detailed plans of the test setup for all tests. To prevent the vertical movement of the transition slab, the head was held vertically by two steel pinned columns (HEA160). For TST2 and TST3, to release the soil's movement behind the back wall and simulate soil settlement, an inclined surface 1:3 (1 m length) was left without backfill under the transition slab close to the back wall. Moreover, to prevent movements at the far end of the pavement, the last two meters of the side walls were roughened for these two tests.

After each test, the pavement, top soil, transition slab and lean concrete were removed and subsequently repositioned before the next test.

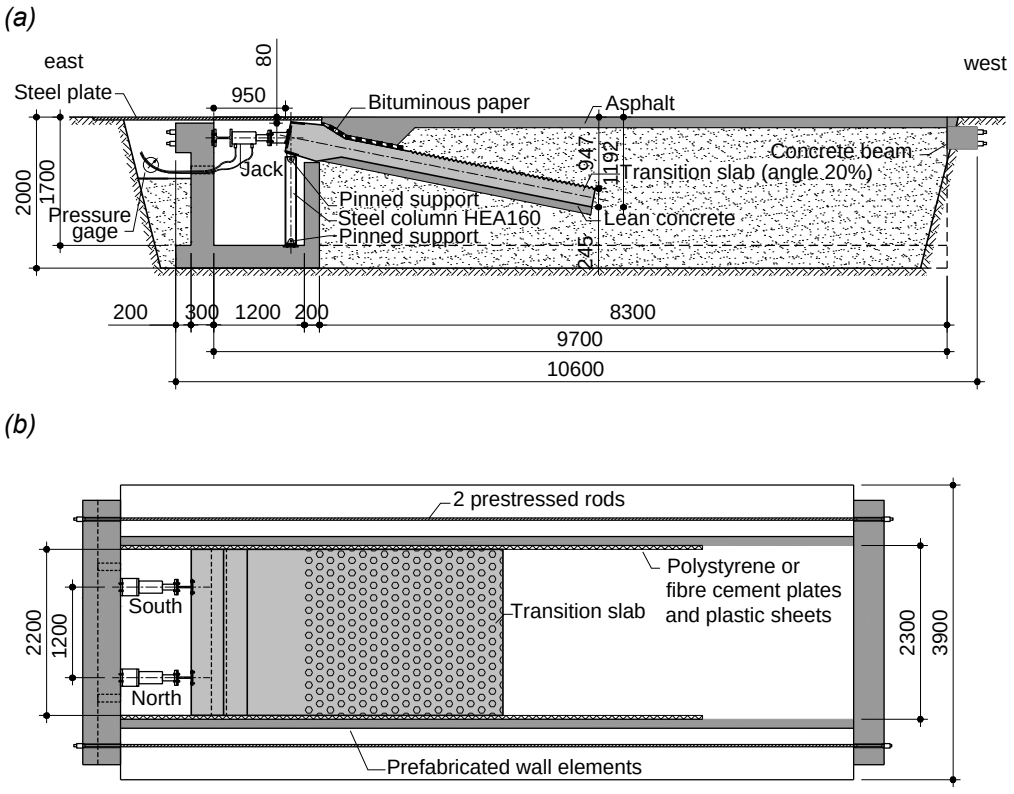

Figure 8: Setup for TST1; (a) Plan view; (b) Longitudinal section

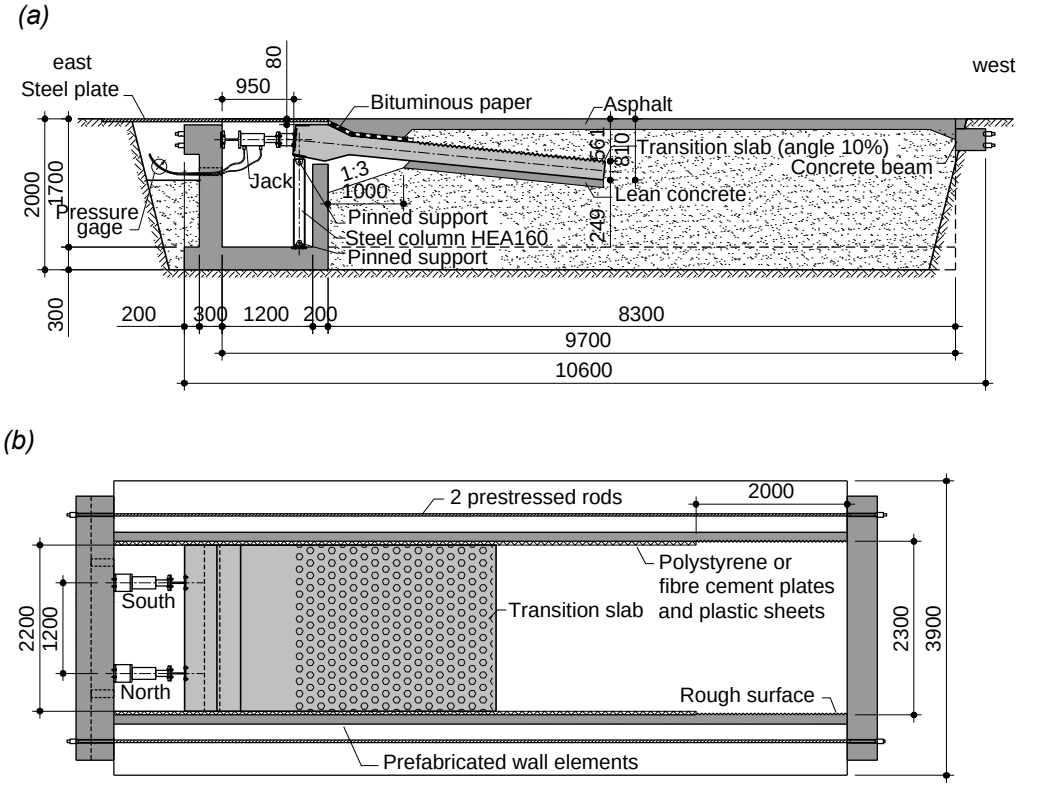

Figure 9: Setup for TST2; (a) Plan view; (b) Longitudinal section

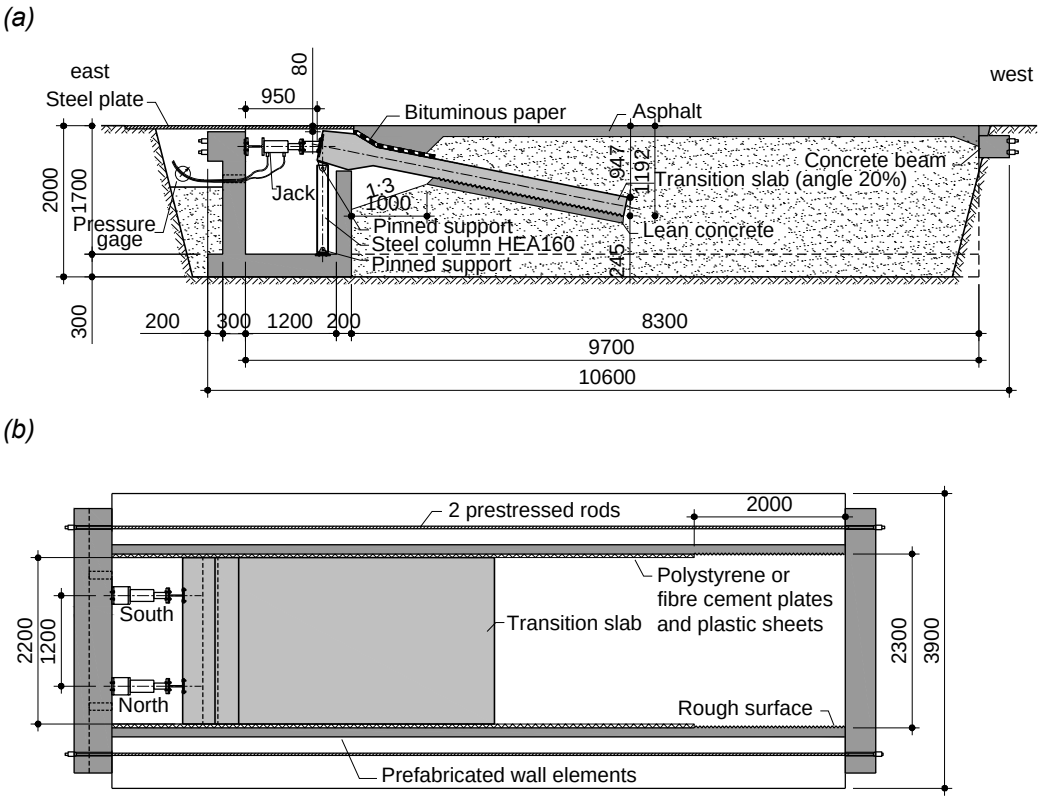

Figure 10: Setup for TST3; (a) Plan view; (b) Longitudinal section

2.2.2 Loadings

Two kinds of loading were applied during the tests:

- Horizontal pulling or pushing of the slab head by hydraulic jacks (Figure 11) to induce a horizontal displacement of the transition slab.

Figure 11: Hydraulic jack acting between the head of the slab (on the left) and the reaction wall (on the right)

- Rolling

To simulate the compacting effect of passing traffic, a pneumatic roller type Ammann (AP 251) was passed over the pavement after each movement phase (20 to 30 passages each time, Figure 12(a)). Figure 12(b) shows the main characteristics of the roller used.

(a)

(b)

Parameter	Value
Weight	20 tons
Operating speed	6 km/h
Distance between axles	3700 mm
Overall rolling width	1800 mm
Wheel width	300 mm
Lateral distance between wheels	200 mm

Figure 12: Compacting of the pavement simulating the effect of passing traffic (a) Amman pneumatic roller; (b) Main characteristics of the roller

2.2.3 Measurements

The following measurements were performed during the tests:

Temperature

- At the bottom of the asphalt layer ($T_{pav,be}$)
- Of the air in the tent (T_{air})

Movements

- Horizontal displacement of the slab head (u_{imp}), the back wall (u_{bw}) and the reaction wall (u_{rw})
- Vertical displacement of the slab head (w_{TS})
- Rotation of the slab head ($\Delta\alpha_{TS}$)
- Longitudinal displacements of the pavement (u_{pav} and $u_{pav,edg}$)

- Vertical displacements of the pavement (w_{pav})
- Location and opening of the cracks in the pavement (x_{crack} , w_{crack})

Force

- Force applied by the hydraulic jacks, through the measure of oil pressure

Table 3 at the end of the present section summarizes all the sensors used on the test specimens.

Thermal measurements

Three temperature sensors of type Pt 100 were used, two (S1 and S2) placed at the bottom of the asphalt layer ACT22S ($T_{pav,be}$) and one measuring the air temperature inside the tent (T_{air}). In addition, for TST1 and TST2, the temperature in the pit between the back wall and the reaction wall was also measured.

Displacement of the transition slab

Two horizontal inductive transducers HBM W100 mm were used to measure the displacement of the slab head (u_{imp}) on the North and South side ($u_{TS,N}$ and $u_{TS,S}$). In addition, two horizontal inductive transducers HBM WA5 mm were installed on both sides of the back wall (u_{bw}). In parallel, an inclinometer WYLER ZEROTRONIC (Type: 3/2 AK-04-055, ± 1°) measured the slab rotation ($\Delta\alpha_{TS}$) of the slab head. Finally, for TST3, a vertical transducer HBM W200 mm was placed on the South side to measure the vertical displacement of the slab head (w_{TS}). The position of the transducers is shown in Figure 13.

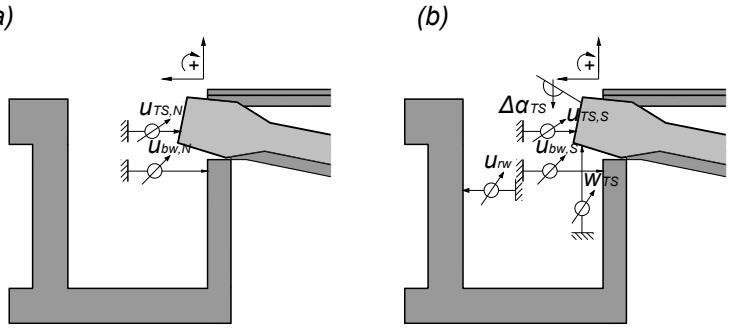

Figure 13: Position of the horizontal and vertical transducers: (a) North side ; (b) South side

For TST1 and TST2, a horizontal transducer HBM WA5 mm measured the displacements of the reaction wall (u_{rw}). This information was not collected for TST3 as the measured values from the first two tests were rather small.

Vertical and longitudinal displacements of the pavement

The instruments used for the measurements of the vertical and longitudinal displacements of the pavement surface (u_{pav} and w_{pav}) were:

- An electronic level Leica DNA 03 with an invar rod for the geodetic levelling.
- A Leica TCR-403 total station (tachymetry) with a stabilized prism (Figure 14).
- A simple ruler for measuring:
  (a) The longitudinal movement at the edges of the pavement (relative displacement between pavement and side walls $u_{pav,edg}$) ;
  (b) The width of the cracks in the pavement (w_{crack}) (Figure 15).

Figure 14: Measurements of longitudinal displacements with a total station

(a) *(b)*

Figure 15: Measurement of (a) the longitudinal displacement between the pavement and the lateral wall; (b) the crack width

Figure 16 shows the position of the measurement points used to follow the vertical and longitudinal displacements of the pavement on three longitudinal axes. In addition, markers were placed on both sides along the edge of the pavement to follow the longitudinal movements at the North (N) and South (S) edges.

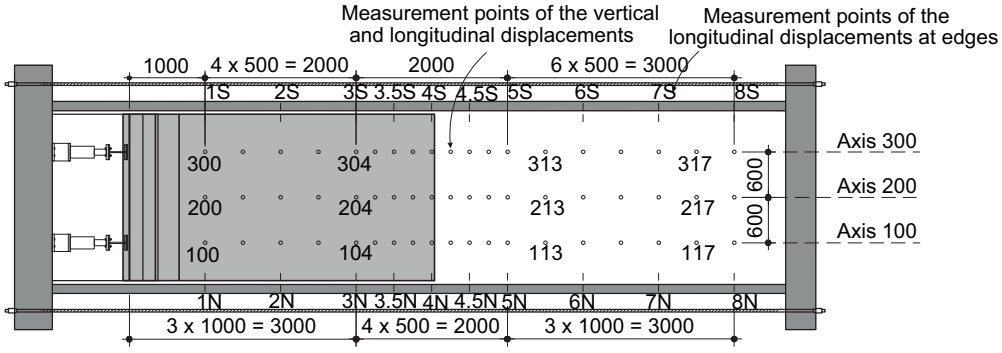

Figure 16: Measurement points for the vertical and longitudinal displacements of the pavement (plan view)

Applied force

The applied force was measured through the oil pressure, with a pressure gauge of type HBM 500 bar. The hydraulic jacks used for the first part of TST1 were of type BIERI with a total capacity of 2 x 200 kN. During the pulling of the first day, the speed of the slab's displacement was very low. For the remainder of the tests, more powerful jacks of total capacity 2 x 400 kN, type ENERPAC were used. The oil pressure in the jacks was measured continuously by an electronic system.

Pavement bending

Measurements of the strains at the bottom of the asphalt layer ACT22S with deformation gauges were also performed (Figure 17). However, the values of the measured deformation due to the passages of the vehicle were small enough (maximum strain 0.3 ‰), so that they were considered negligible in comparison with the strains caused by the pulling and pushing phases of the transition slab and are not reported.

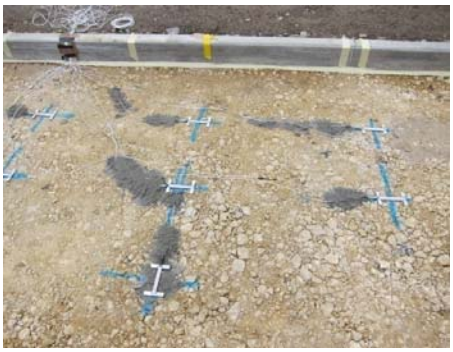

Figure 17: Asphalt strain sensors in position before placing the asphalt layers

Table 3: Technical characteristics of the sensors

Measure	Instrument	Type	Measuring range
Temperature	Thermocouple sensors	Pt100	+ 200 °C
Displacements	Inductive transducers	HBM W100 HBM WA5 HBM W200	± 100 mm ± 5 mm ± 200 mm
	Electronic level	DNA 03 Leica	1.80-110 m
	Electronic total station with stabilized prism	TCR-403 Leica	
	Ruler		
Rotation	Inclinometer	WYLER ZEROTRONIC: (3/2 AK-04-055)	± 1° (17.45 mRad)
Force	Pressure gauge Hydraulic Jacks	HBM 500 bar BIERI & ENERPAC	0 - 500 bar 200 kN & 400 kN

2.3.4 Sequence of operations

For all tests, the initial levelling (and tachymetry for TST1 and part of TST2) of the pavement surface was followed by iterations of:

- Imposing a displacement to the slab by pushing or pulling with a constant rate until the target value was reached.
- Compacting of the soil by passing the roller.
- Levelling (and tachymetry) of the pavement surface. Recording the longitudinal displacements at the edges of the pavement.

The displacement sequence for each test concerning the loading of the slab, is given in Table 4.

Figures 18 to 20 show the sequence of operations (loading and measurement procedure) for each test. Appendix F contains the detailed sequence of operations for each test, together with the measurement results.

Table 4: Displacement sequence of the slab head

	Sequence	u_{imp} [mm]
TST1	Pulling	+20, +40, +60, +77
	Pushing	+40, +8, -11, -30
TST2	Pulling	+20, +40, +60, +77
	Pushing	+40, 0, -20, -40, -60
	Pulling	-20, 0
TST3	Cycles (pushing then pulling)	1: -20 to +20 2: -24 to +30 3: -30 to +30

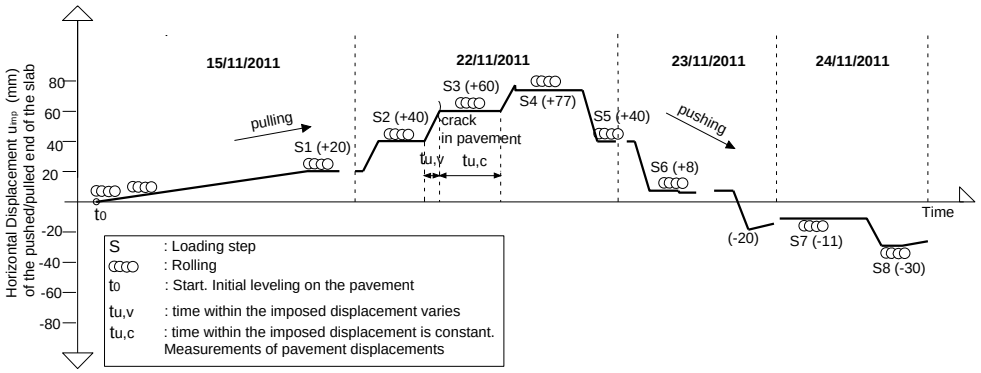

Figure 18: Load steps and measurement sequence for TST1

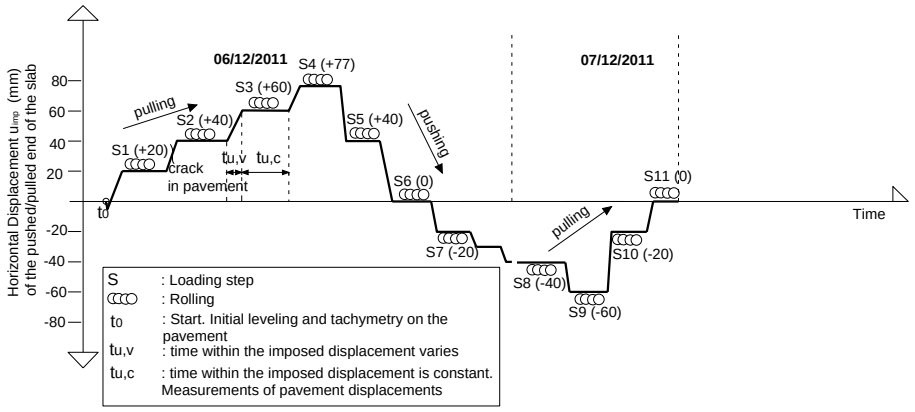

Figure 19: Load steps and measurement sequence for TST2

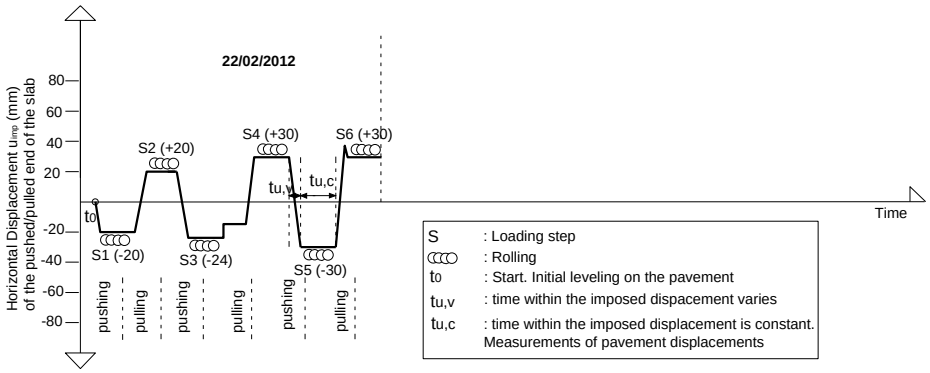

Figure 20: Load steps and measurement sequence for TST3

3 Results and interpretations

This chapter presents the main results for the three tests. Positive values for the forces and horizontal displacements indicate values in the direction of pulling the slab. For vertical displacements, positive values indicate an upward movement. The positive rotation of the slab head is defined in Figure 13.

3.1 Temperature

The values obtained by the temperature sensors in the asphalt (S1, S2) for tests TST1, TST2 and TST3 are presented in Figures 21, 22 and 23 respectively. The pit temperature (available only for TST1 and TST2) was much less affected by the heating system and is thus representative of the soil temperature at a larger depth. The average temperature below the pavement ranges between from 15°C to 20°C for TST1, from 15°C to 25°C for TST2 and is about 6°C for TST3.

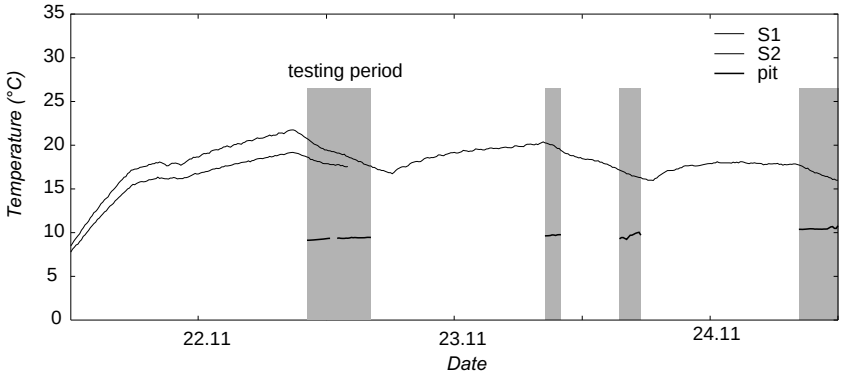

Figure 21: Temperature measurements during TST1

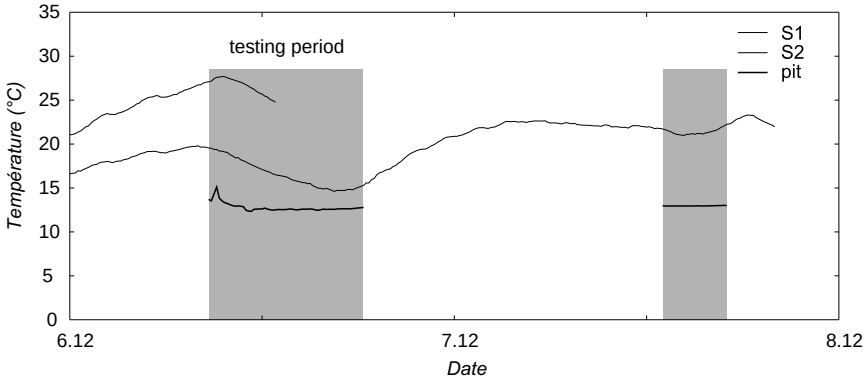

Figure 22: Temperature measurements during TST2

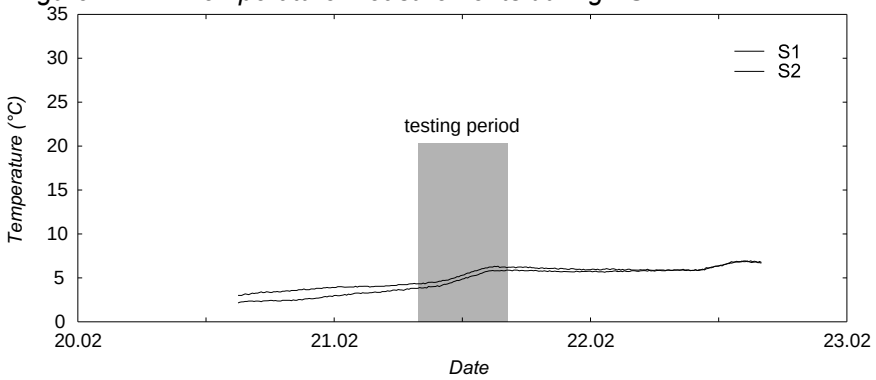

Figure 23: Temperature measurements during TST3

3.3 Imposed displacement and applied force

Figure 24 shows, for each test, the applied force at the slab head required to reach the specified displacement for each movement phase. The force required to move the transition slabs with a larger inclination (20 %, TST1 and TST3) was signify-cantly larger than that needed to move the slab TST2 with an inclination of 10 %.

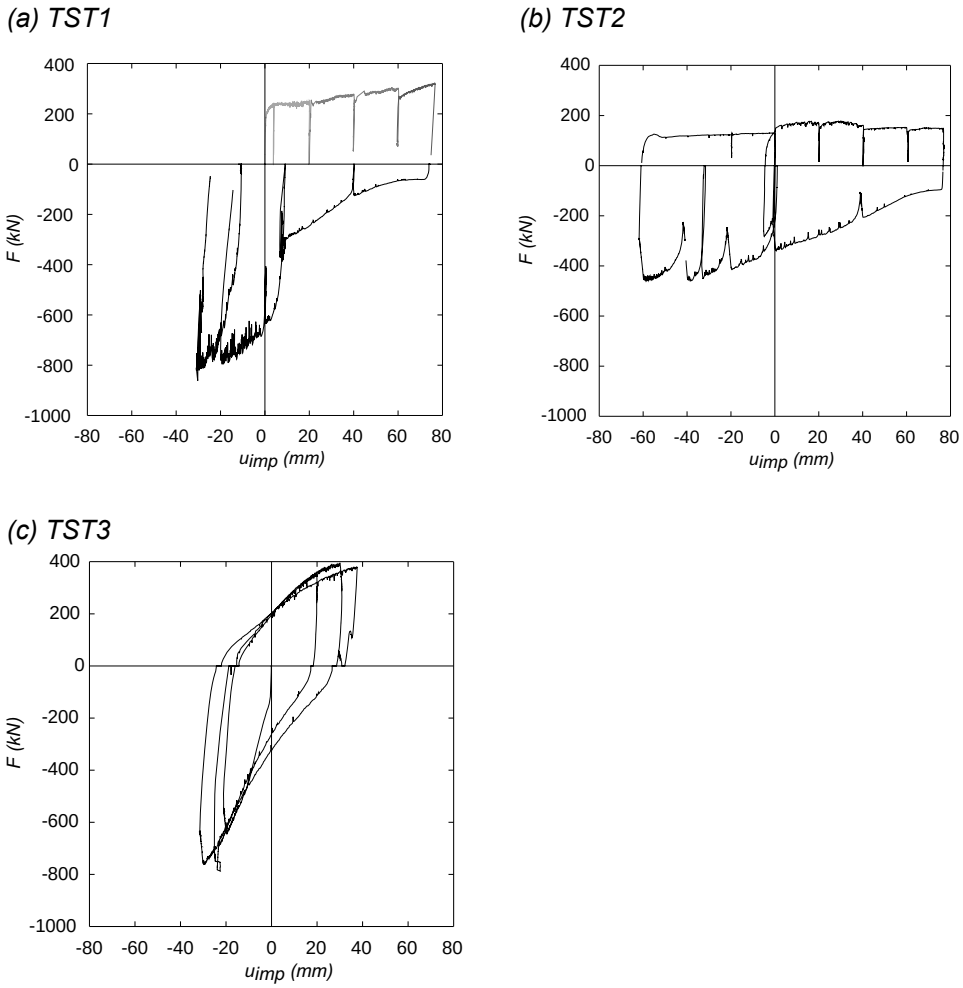

Figure 24: Force (F) - Imposed Displacement (u_{imp})

In pulling the slab, the target value of displacement of 80 mm was almost reached with specimens TST1 and TST2 (77 mm). These tests were stopped because of mechanical limitations of the setup. In both cases, very large cracks had opened in the pavement before the maximum displacement was reached. Once the move-ment was initiated, no significant increase in force was required to reach larger dis-placements. The force required to move slab TST3, with the rough surface at the bottom, was approximately 25 % larger than to move slab TST1, with a smooth bot-tom surface.

In pushing, the force required to move the slab was more than twice that required in pulling. The position of the rough surface of the slab does not appear to play a sig-nificant role. Slab TST2 with a small inclination reached the target value of 60 mm, but the other two slabs did not, as the maximum force that could be applied, 800 kN, was not sufficient.

The cycles performed in TST3 showed a tendency for the load needed to move the slab in tension to slightly diminish with increasing cycle count, while the load need-ed to move it in compression slightly increased.

Table 5 gives the maximum and minimum values of the force applied for each test.

Table 5: Maximum force for all three tests

	Pulling	Pushing
	$F^+ max$ [kN]	$F^- max$ [kN]
TST1	320	-860
TST2	180	-460
TST3	400	-800

3.4 Rotation of the slab head

Figure 25 shows the rotation of the slab head and the corresponding applied force for each test.

In pulling, the slab head rotation is negative. A steeper inclination (TST1 and TST3) leads to more than doubling the values of slab rotation compared with a flatter one (TST2). For the same u_{imp} = 20 mm, the rotation of the slab is larger in TST3 with a rough bottom surface, than in TST1, indicating bending of the slab during TST3. This may also be due to the removal of the soil in the vicinity of the back wall for TST3.

In pushing, the rotation of the slab head is positive. A steeper inclination (TST1 and TST3) leads to much larger values of the slab rotation than a flatter one (TST2), independently from the roughness of the bottom surface of the slab.

(a)TST1

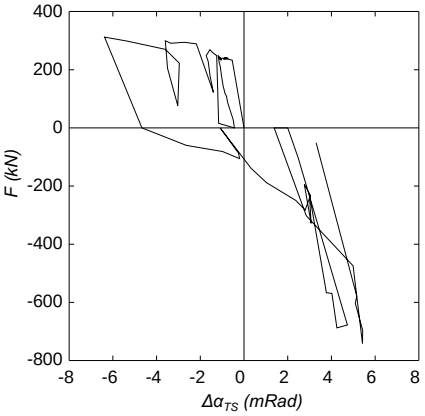

(b) TST2

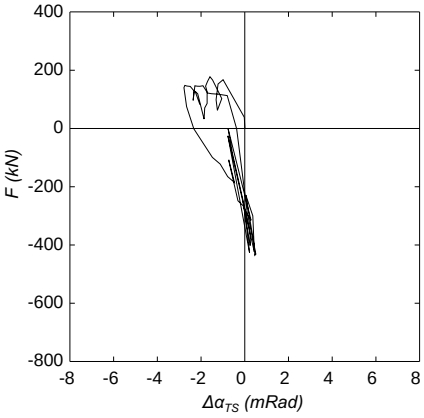

(c) TST3

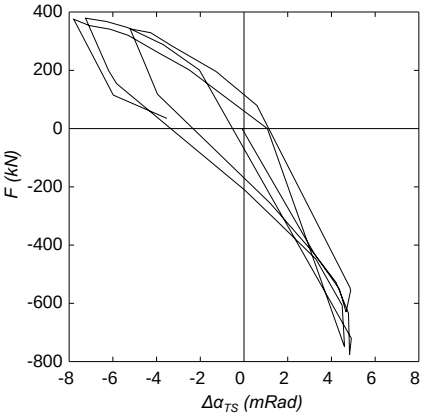

Figure 25: Force - Rotation diagrams

3.5 Horizontal displacement of the back wall

Figure 26 shows the horizontal displacement of the top of the back wall. Large displacements (max u_{bw} = 2.8 mm) were recorded at the end of the pulling phase of TST1 (u_{imp} = +77 mm), indicating significant pressure on the back wall. For TST2 and TST3, the space left without backfill under the transition slab close to the back wall (Figures 9 and 10) sharply decreased the wall's movement.

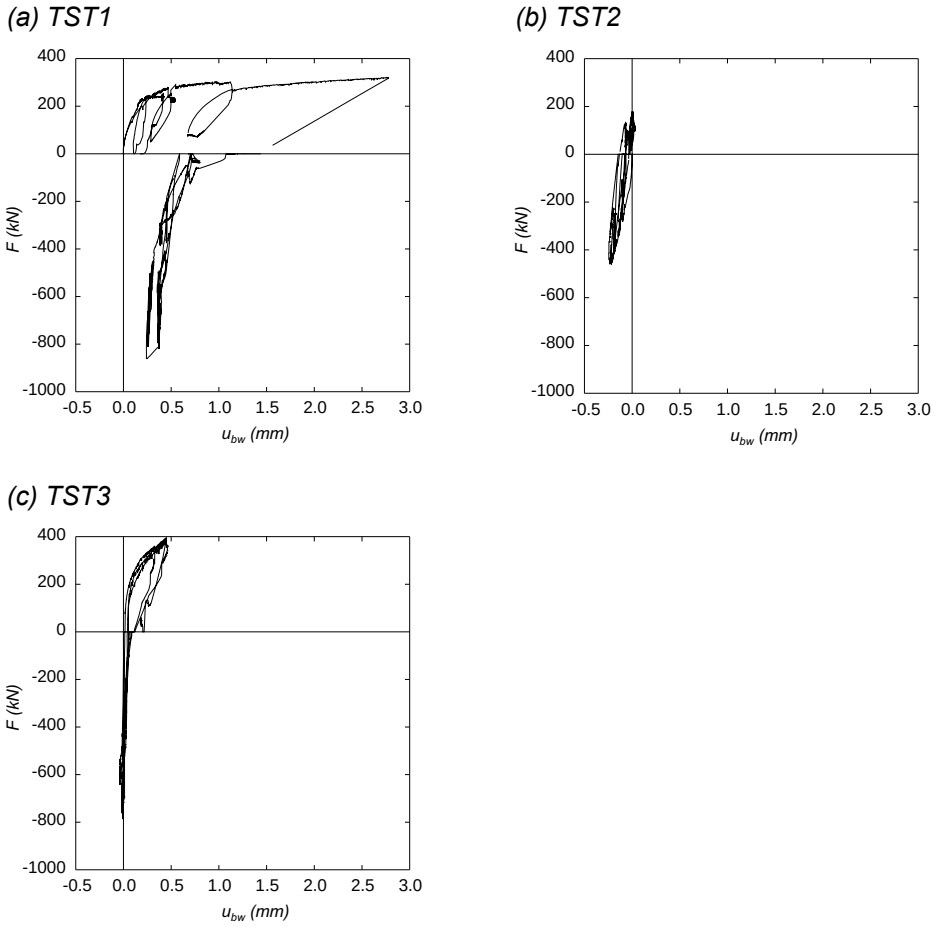

Figure 26: Force (F) - Horizontal displacement of the back wall (u_{bw})

3.6 Vertical displacement of the slab head

Figure 27 shows the vertical displacement of the slab head during TST3. The large increase in force for a constant vertical displacement (w_{TS} = +15.5 mm) occurred during pushing, due to the activation of the restraint provided by the vertical HEA160 columns in tension. Vertical movements were free to occur between approximately -5 and + 15 [mm] due to gaps in the connections at the top and the bottom of the steel columns.

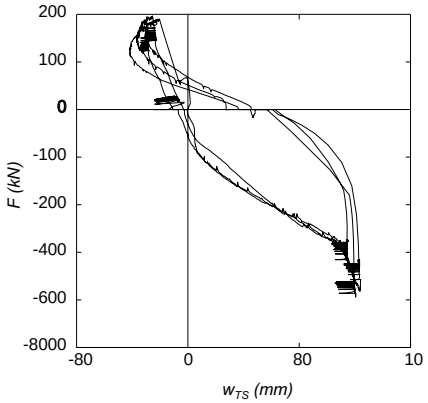

Figure 27: Force (F) - Vertical displacement of the slab head (w_{TS}) in TST3

3.7 Movements of the pavement in the pulling phase

Figure 28 shows the vertical and longitudinal displacements at the edges of the pavement in the pulling phase, as a function of the distance *x* from the bridge end. The axis with the largest vertical displacements is shown for each test. Appendix E gives the vertical displacements of the pavement along all measurement axes.

Vertical movements of the pavement in tension

As shown in Figure 28, the behaviour of the pavement in the pulling phase was similar in TST1 and TST2. Over the entire length of the transition slab, it moved upwards by Δw_{pav} because the slab slid upwards on its bedding. Above the end of the transition slab, a sharp pit was observed.

A different movement of the pavement was observed in TST3. On the bridge end of the slab, it moved slightly downwards and above the last third of the slab's length, a bump was observed. After the end of the transition slab a slight pit was formed.

Table 6 and 7 summarises characteristic values from the diagrams of Figure 28.

Table 6: Maximum ("pit") vertical displacements of the pavement in pulling

	Axis	*x* (m)	u_{imp} (mm)	w_{pav} (mm)
TST1	200	4.00	77	-9.8
TST2	300	4.25	77	-13.8
TST3	100	5.00	20	-0.3

Table 7: Upward movement of the pavement above the transition slab in TST1 and TST2 during pulling

	Axis	*x* (m)	u_{imp} (mm)	Δw_{pav} (mm)
TST1	200	3.25	20	4.0
			40	4.8
			60	5.0
			77	1.3
TST2	300	3.50	20	2.8
			40	2.3
			60	2.1
			77	2.1

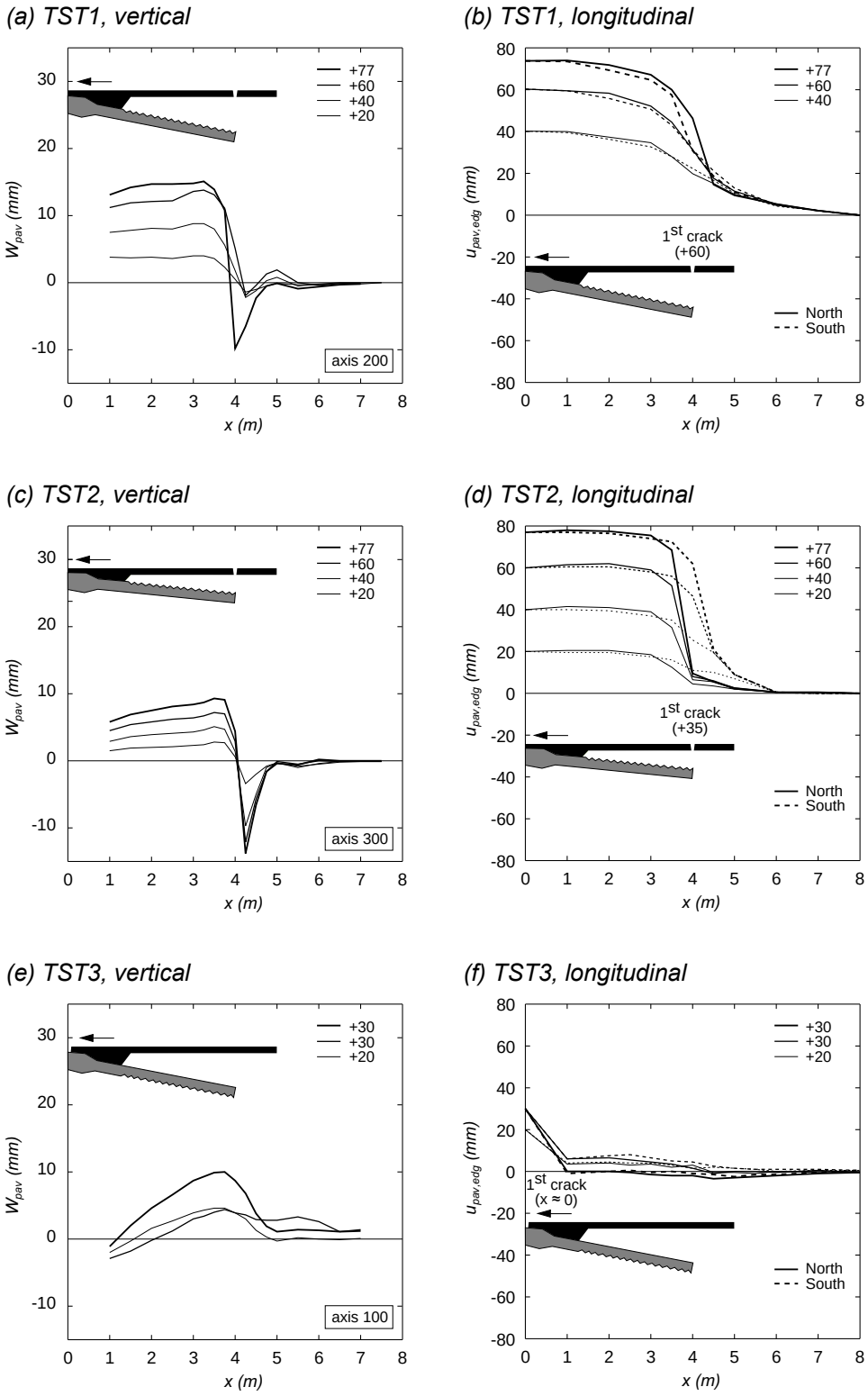

Figure 28: Vertical and longitudinal displacement of the pavement in tension (load steps refer to the imposed displacement u_{imp})

Longitudinal movements of the pavement in tension

As shown in Figure 28, for TST1 and TST2 the longitudinal strains in the pavement were concentrated in a limited area at the end of the slab (between x = 3.50 and x = 4.50 m). For TST1, the cracks appeared for u_{imp} = 60 mm at 3.50 m < x_{crack} < 4.00 m on the South side and 4.00 m < x_{crack} < 4.50 m on the North side, Figure 29(a)).

The strain developed earlier for TST2, resulting in cracks for u_{imp} = 35 mm (3.50 m < x_{crack} < 4.00 m at the North side and 4.00 m < x_{crack} < 4.50 m at the South side, Figure 29(b)). The soil above the slab moved together with it because of the rough top surface of the transition slab, $u_{pav,edg} \sim u_{imp}$).The pavement behind the crack (x > 4.50 m) had small horizontal displacements.

For TST3, the longitudinal strains in the pavement were very small, because a separation between the pavement and the transition slab occurred very early in the pulling phase (x = 0 m, Figure 29(c)), probably because of the low friction between the smooth top surface of the transition slab and the soil above it.

(a) TST1

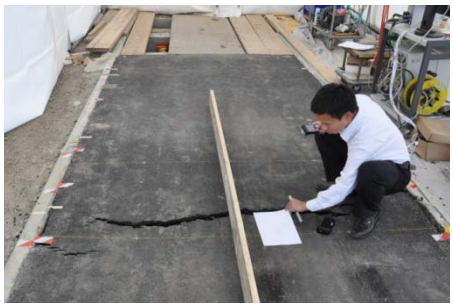

(b) TST2

(c) TST3

Figure 29: Crack in the pavement during pulling: (a) above the end of the transition slab in TST1 (3.50 m < x_{crack} < 4.50 m); (b) above the end of the transition slab in TST2 (3.50 m < x_{crack} < 4.50 m); (c) at the bridge end of the transition slab in TST3 (x_{crack} = 0 m)

3.8 Movements of the pavement in the pushing phase

Figure 30 shows the vertical and longitudinal displacements of the pavement in the pushing phase, as a function of the distance *x* from the bridge end.

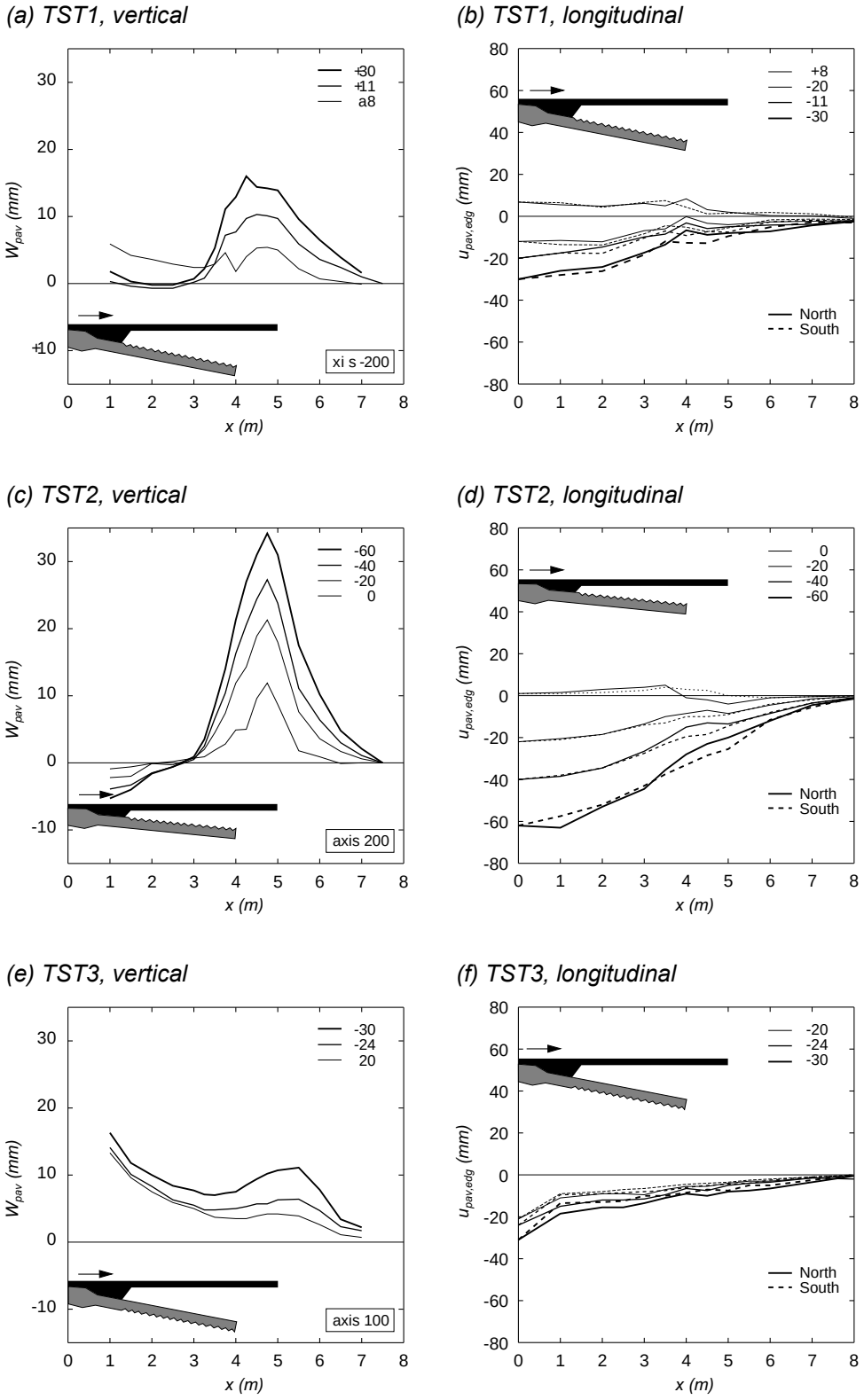

Figure 30: Vertical and displacement of the pavement in compression

Vertical movements of the pavement in compression

As shown in Figure 30, in TST1 and TST3 the pavement moved upwards on the bridge side of the slab and a bump was observed after the end of the transition slab, further away for TST3. In TST2, the pavement moved slightly downwards on the bridge side of the slab, while a sharp and high bump was observed after the end of the transition slab. Table 8 gives the maximum value and the location of the bump for all three tests.

Table 8: Position and amplitude of the bump in the pavement in the pushing phase

	Axis	x (m)	u_{imp} (mm)	w_{pav} (mm)
TST1	200	4.25	-30	16.0
TST2	200	4.75	-60	34.2
TST3	100	5.50	-30	11.1

Longitudinal movements of the pavement in compression

As shown in Figure 30, for TST1 and TST2, the longitudinal displacements of the pavement decrease almost linearly from values close to u_{imp} (x = 1.00 m) to zero (x = 8.00 m). The pavement above the slab moved together with it in the pushing phase, closing the cracks opened in the pulling phase. In TST3, the longitudinal strains in the pavement were smaller because of the separation of the pavement that happened in a previous pulling phase.

3.9 Movements of the pavement in the final pulling phase of TST2

Figure 31 shows the vertical and longitudinal displacements of the pavement in TST2, in its final pulling phase, back to zero displacement at the slab head.

(a) Vertical *(b) longitudinal*

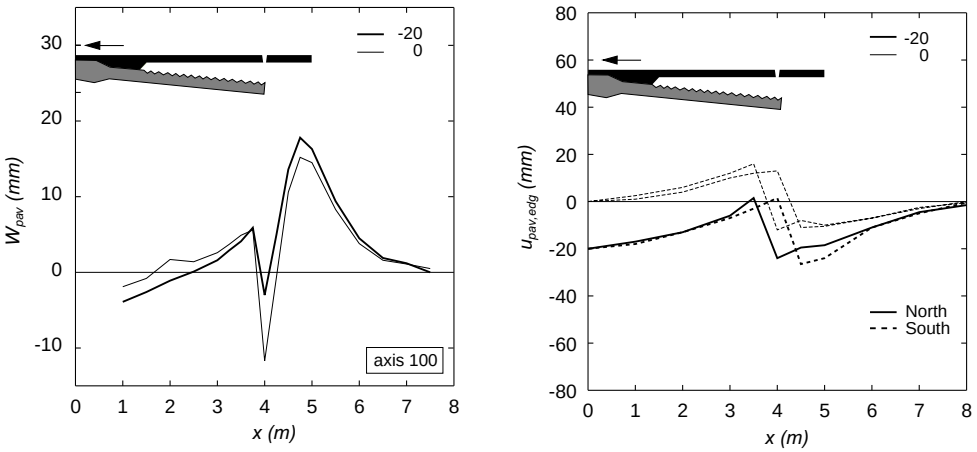

Figure 31: Displacement of the pavement in the final pulling phase of TSTS

Both a pit and a bump remained in the pavement, as well as longitudinal strains mainly around the end of the transition slab. This behaviour indicates that the pavement deformed plastically before cracking. Notice also that the two sides of the crack are vertically offset in the final position, which would have an effect on the comfort of users.

3.10 Maximum vertical displacements in the pavement

Figure 32 shows the maximum vertical displacements of the pavement at two critical points. Point A refers to the maximum negative displacement (pit), while point B refers to the maximum positive displacement (bump) during various phases of each test.

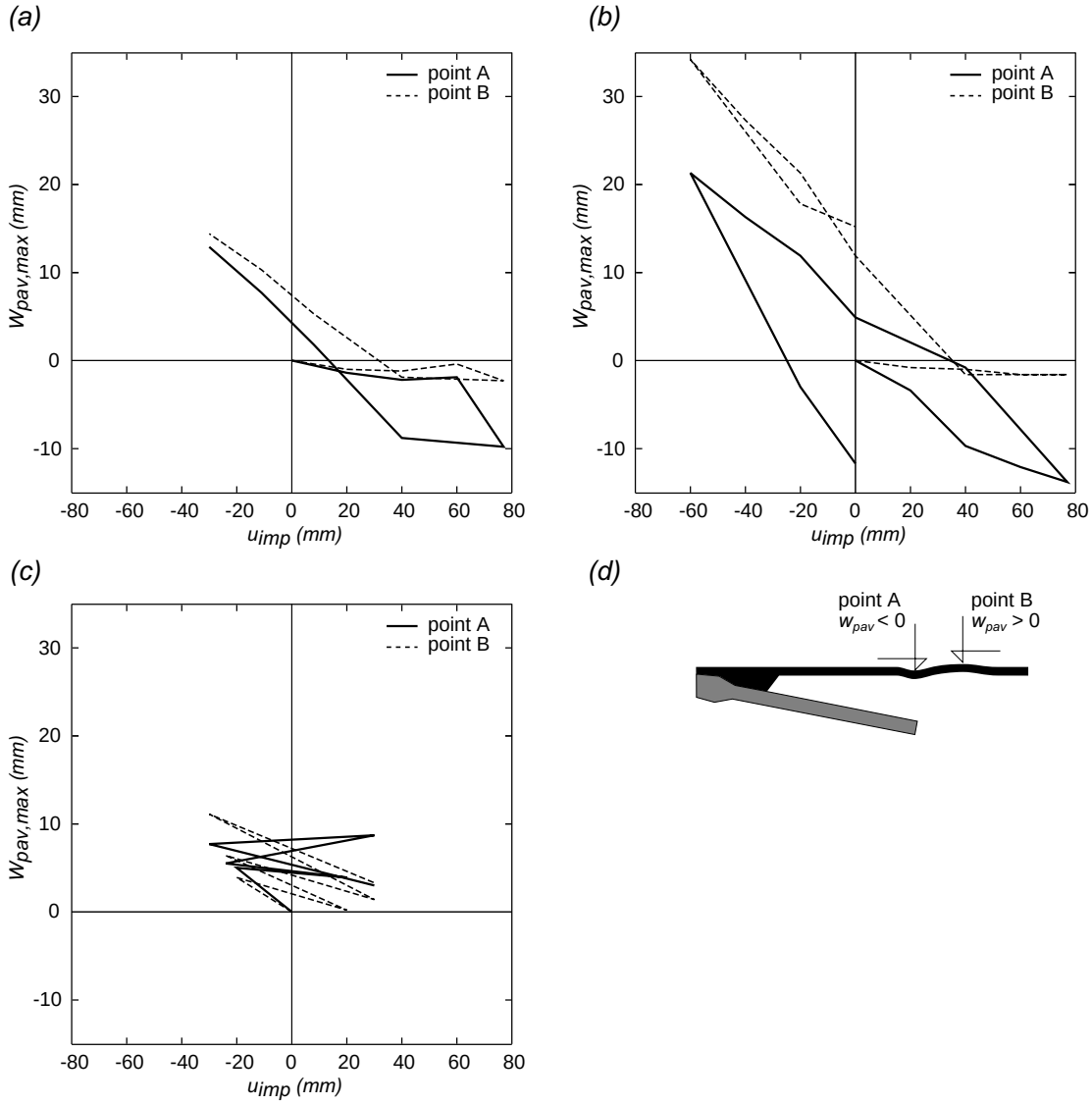

Figure 32: Maximum vertical ($w_{pav,max}$) displacement of the pavement at the point of the pit and bump - Imposed displacement (u_{imp}): (a) TST1; (b) TST2; (c) TST3; (d) detail of the points

3.11 Kinematics of the transition slab

3.11.1 Kinematics in the pulling phases

In the pulling phase, three types of slab kinematics were observed. If the uplift of slab head was not prevented, the slab started to slide upwards on its bedding (Figure 33). This was the dominating behaviour for the pulling phase of TST1 and TST2 (slabs with smooth bottom surface), as the connections to the steel columns allowed some slipping. The following observations were made:

- The pavement directly above the slab moved upwards as a rigid body by Δh (Figure 33)
- A sharp pit was observed above the end of the transition slab (Figure 28 (a) and (c)).
- The horizontal strains in the pavement were concentrated in a small zone at the end of the transition slab (Figure 28 (a) and (c)), indicating that the soil over the slab moved together with it.
- The pulling force did not depend on the total displacement (Figure 24 (a) and (b)). It is more related to friction (plastic behaviour of slab-soil interface) and displacement velocity (viscous behaviour of the pavement).

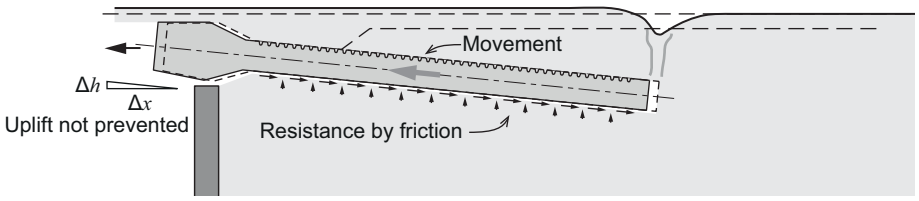

Figure 33: Kinematics 1: Sliding of the slab in tension

If the uplift of the slab was prevented so that the slab could not slide upwards on its bedding, the pressure on the wall and its displacement increased considerably (Figure 34). This kind of behaviour had an influence on the latter pulling phases of TST1 (u_{imp} = +60 mm to u_{imp} = +77 mm), when the connection to the steel columns was not slipping any more. The main differences compared to the previous observations are:

- The upwards movement of the pavement above the transition slab was smaller (Δw_{pav} = 1.3 mm for x = 3.25 m, Table 7 and Figure 28 (a)).
- The displacement of the back wall increased (Figure 26 (a)).
- The resistance to pulling was larger and more dependent on the total displacement (Figure 24 (a), between +60 and +77 mm).

If this kind of kinematics is assumed, the resistance to the movement of the slab is generated by the compressibility of the soil and the stiffness of the back wall.

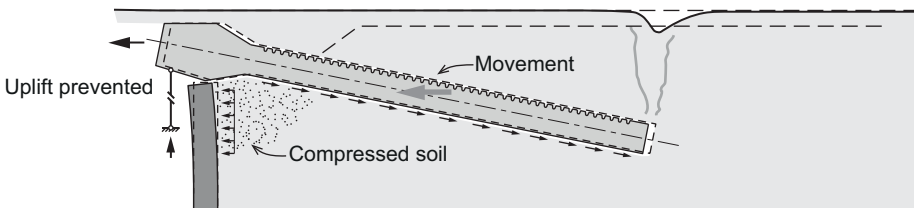

Figure 34: Kinematics 2: Movement of the slab if the uplift of the bridge end of the transition slab is restrained

A third type of kinematics was observed in TST3 with the rough bottom surface. The main differences compared to the previous tests were:

- The uplift of the pavement was the largest above the last third of the transition slab (Figure 35).
- The displacement of the back wall was small, similar to TST2 (Figure 26 (c)). This was probably due to the space left without backfill under the bridge end of the transition slab.
- The force required in the pulling phase was approximately 25% larger than for TST1 (Table 5).
- For the same u_{imp} = 20 mm, the rotation of the slab is much larger than for TST1 (Figure 25 (a) and (c)).

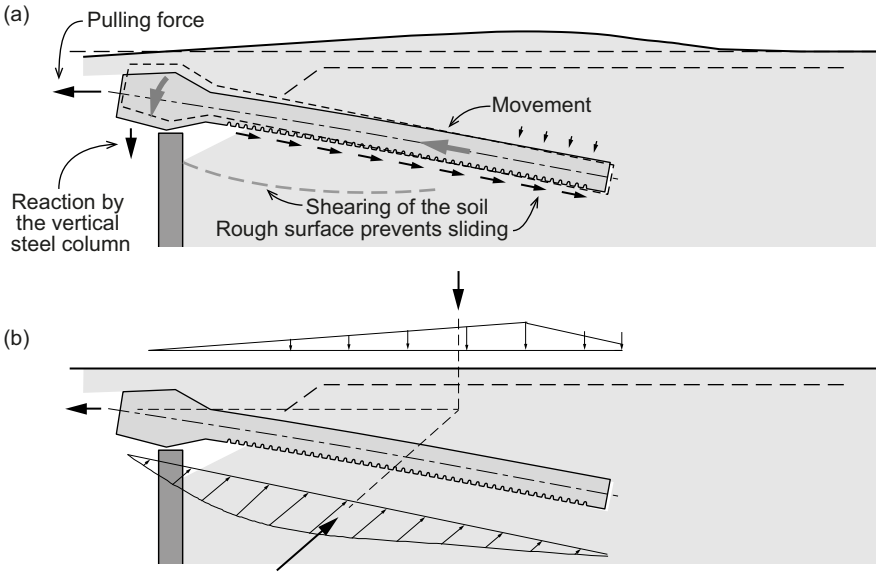

Figure 35: Kinematics 3: (a) Downwards bending of the transition slab if its rough bottom surface or a stiff back wall prevents it from sliding; (b) equilibrium of forces

These observations indicate that the rough bottom surface of the slab prevents it from sliding, so the movement has to occur by shearing of the soil. The lever arm of the pulling force (and the vertical reaction provided by the steel columns) applies a large flexural moment on the slab, pulling the slab head downwards (negative rotation). This is also clear when considering the movement of the pavement at the bridge end of the transition slab (Figure 28 (e) and Figure 35).

3.11.2 Kinematics in the pushing phases

In the pushing phases, the kinematics mostly depends on the inclination and the smoothness of the bottom surface of the transition slab. Two kinds of behaviour can be distinguished.

In TST2 (α_{TS} = 10%), the following observations were made:

- The pavement moved slightly downwards at the bridge end and considerably upwards behind the end of the transition slab, the highest point being at approximately 1 m from the end of the transition slab (w_{pav} = 34.2 mm for x = 4.75 m, Figure 30 (c) and Table 8).
- The force required in pushing was more than two times larger than the force in pulling (Table 5).
- The rotation of the slab head was small (Figure 25 (b)).

Based on the observations, it can be inferred that the slab was sliding downwards on its bedding without significant deformations of the slab itself (Figure 36). The additional resistance to compression compared to that in tension arises from the passive soil pressure at the end of the transition slab.

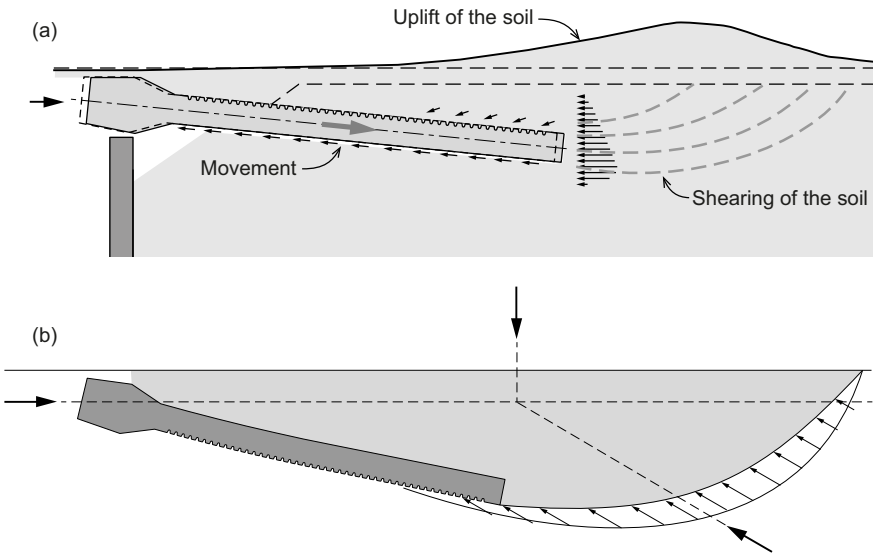

Figure 36: Kinematics 4: (a) Movement of a sliding slab in a pushing phase; (b) equilibrium of forces

In the case of α_{TS} = 20% (TST1 and TST3):

- The pavement above the bridge end of the slab moved upwards (Figure 30 (a) and (e)).
- The bump behind the end of the transition slab was further from the slab than for the previous case, if the soil was unaffected by the preceding pulling phase (w_{pav} = 11.1 mm for x = 5. 50 m in TST3, Figure 30 (e) and Table 8).
- The force required in the pushing phase was up to 800 kN (Figure 24 (a) and (c)) and it did not depend notably on the roughness of the bottom surface of the slab.
- The slab head rotated upwards (positive rotation), in the same manner for both types of bottom surfaces (Figure 25 (a) and (c)).

For the steeper slab inclination, the passive soil pressure for the slab was significantly larger than for the smaller one, because the end of the transition slab was deeper in the soil. Correspondingly, the passive failure zone in the soil was larger. The friction on the underside of the slab had a smaller influence on the total resistance. The slab underwent significant flexural deformations, as also the lever arm between the pushing force and the passive earth pressure was larger than for the previous case (Figure 37).

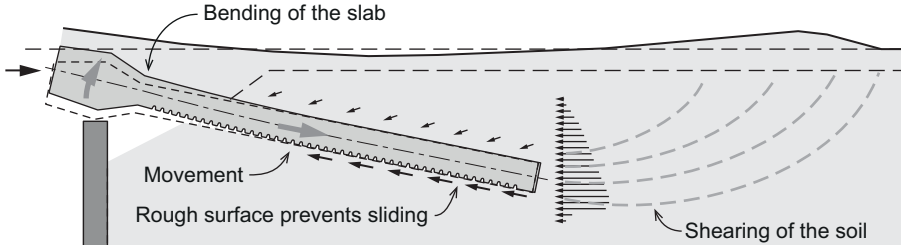

Figure 37: Kinematics 5: Movement of the slab if the slab cannot slide

3.12 Movements of the transition slab

As was already mentioned, the vertical displacement of the slab head was measured only for TST3. Nevertheless, considering that the vertical movement of the pavement at x = 1 m is representative of the slab's head vertical displacement for TST1 and TST2, Figure 38 gives the vertical displacement of the slab as a function of the imposed horizontal displacement for the three tests.

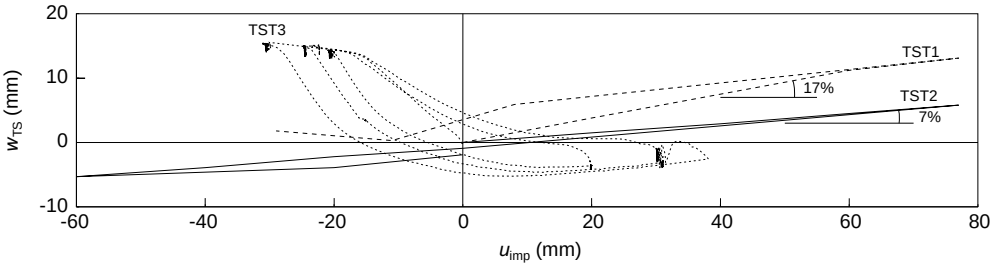

Figure 38: relationship between the vertical (w_{TS}) and horizontal displacement (u_{imp}) of the slab head

The following observations can be made from Figure 38:

- The inclination of the curves in TST1 and TST2 is similar to that of the transition slab (20% and 10%), indicating that the slab was sliding on its bedding (Figures 33 and 36).
- During the pushing phase of TST1, the slab was sliding down but it was also significantly bending upwards at the same time (Δw_{TS} /Δu_{imp} smaller than the inclination of the slab).
- In TST1 and TST2, with the smooth surface at the bottom of the slab, the pulling force ($u_{imp} > 0$) moved the slab head upwards and the pushing force ($u_{imp} < 0$) moved it downwards. In TST3, with the rough surface at the bottom of the slab, the above observations are reversed. This is probably due to bending of the slab.
- In every cycle of TST3, almost the same vertical displacement of the slab was achieved in tension and compression respectively because of the activation of the steel columns during the large imposed displacements.
- The maximum vertical displacement of the slab head were observed in TST3 (w_{TS} = 15.5 mm) in the pushing phases.
- In TST3, the amplitude of the horizontal displacement of the slab u_{imp} was limited by the maximum force of the jacks. The displacement reached was quite small in comparison with TST1 and TST2. The rough bottom surface prevented sliding and caused bending of the slab (Figures 35 and 37).

3.13 Strains in the pavement

Table 9 shows the measured strain in the pavement for tests TST1 and TST2. The maximum strain in the pavement before cracking, at $u_{imp} < 60$ mm for TST1 and at $u_{imp} < 35$ mm for TST2, was approximately $\varepsilon_{pav,edg} = 0.016$ for both tests. Assuming a linear relationship between maximum strain and horizontal displacement, the tensile strain in the pavement just at the initiation of the first crack can be calculated as: $16.3 \times \frac{60}{40} \approx 24$ ‰ for TST1 and $16.0 \times \frac{35}{20} \approx 28$ ‰ for TST2. Asphalt has some strain capacity as a consequence of its viscoelasticity, which is also temperature-dependent (10°C to 15°C for TST1 and TST2).

Table 9: Strain in the pavement in tension during TST1 and TST2 (the shaded cells indicate the location of the cracks)

	u_{imp} [mm]	40	60	77
	x [m]	$\varepsilon_{pav,edg}$ (‰)		
North edge **TST1**	1	2.7	1.2	2.2
	2	2.7	6.2	4.7
	3	13.3	15.3	14.3
	3.5	**16.3**	26.3	27.3
	4	9.3	27.3	63.3
	4.5	10.3	12.3	10.3
	5	5.2	6.2	4.2
	6	2.7	3.2	3.2
	7	2.2	2.2	2.2
		Before	*After*	
		Cracking		

	u_{imp} [mm]	20	40	60	77
	x [m]	$\varepsilon_{pav,edg}$ (‰)			
North edge **TST2**	1	0.0	0.0	0.0	0.0
	2	0.0	0.5	-0.5	0.5
	3	2.0	2.0	3.0	2.0
	3.5	12.0	15.0	15.0	14.0
	4	**16.0**	50.0	87.0	118.0
	4.5	2.0	2.0	4.0	8.0
	5	3.0	7.0	7.0	6.0
	6	1.5	1.5	2.0	2.0
	7	0.0	0.0	0.0	0.0
		Before	*After*		
		Cracking			

Figure 39 shows the strain in the pavement for TST1 and TST2, just before the cracks appeared. Due to the smaller inclination of TST2, the strains were concentrated in a smaller area (Figure 28 (a) and (c)). As a result, the limit strain was reached for a smaller displacement of the slab than for TST1.

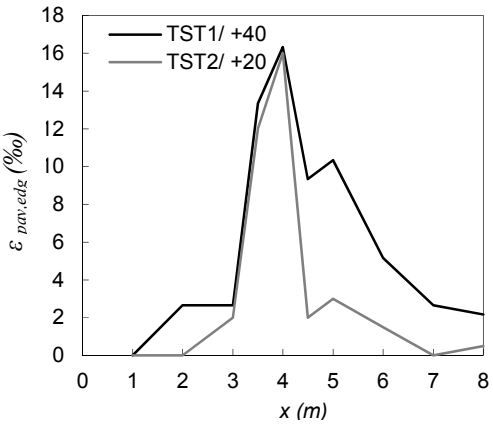

Figure 39: Strain in the pavement ($\varepsilon_{pav,edg}$) - Distance from the bridge end (x)

Based on the two measurements of slabs TST1 and TST2 shown in Figure 39, a direct relationship can be established between the maximum strain in the pavement $\varepsilon_{pav,edg}$ and the buried depth at the end of the transition slab $e_{TS,extr}$:

$$\varepsilon_{pav,edg} \approx \frac{0.3 \cdot u_{imp}}{e_{TS,extr}} \qquad (3)$$

This tentative relationship needs to be checked against additional experimental data.

4 Conclusions and practical considerations

The three tests performed show that the buried depth at the end of the transition slab, its inclination and the roughness of its surfaces in contact with the soil play an important role on the behaviour of the pavement. These observations lead to the following practical conclusions for bridges without expansion joints (integral bridges without mechanical bearings or semi-integral bridges with mechanical bearings). It must be noted in preamble that some of the phenomena described in this chapter have not yet been reported and may only appear under extreme circumstances, as were investigated in the present test series.

a) Connection between the bridge and the transition slab

The experimental results show that the imposed displacements due to the deformation of the bridge can produce large forces on the joint between the bridge end and the transition slab. These forces are not only longitudinal, but can also have a vertical component. If these vertical internal forces cannot be resisted, this results in an important vertical displacement of the pavement above the transition slab. The detail shown in Figure 40(c) should therefore be avoided because it could not resist the horizontal and vertical forces induced by the movement at the bridge end. In addition, the details of Figures 40(b) and (c) should be thoroughly checked concerning the distribution or internal forces. If the detail shown in Figure 40(a) is subjected to a shortening of the bridge, this will lead to a large tensile force, but also an upward shearing force in the concrete hinge, which can lead to the separation between the transition slab and the short corbel with a potential local failure.

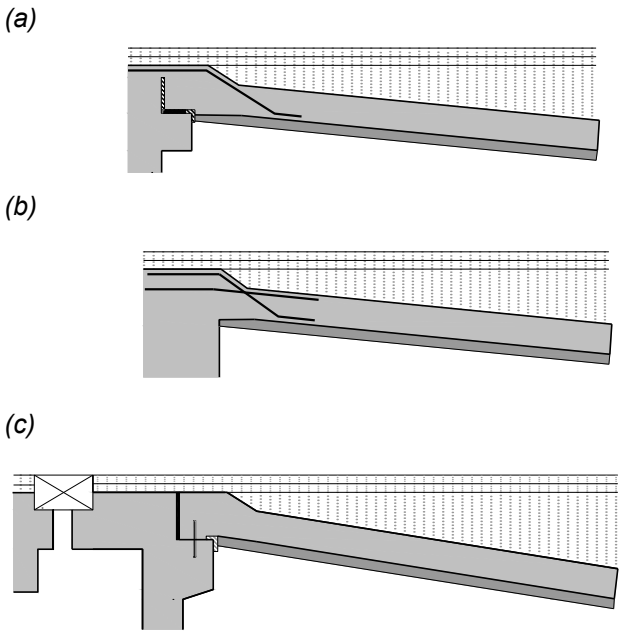

Figure 40: Connection details between abutment and transition slab: (a) detail recommended by FEDRO [OFROU 2011] for integral and semi-integral abutments; (b) new improved detail for standard and integral abutments [DREIER 2011]; (c) detail for standard abutments with expansion joints according to FEDRO [OFROU 2011]

b) Buried depth at the end of the transition slab

The buried depth at the end of the transition slab $e_{TS,extr}$ is an important parameter that can have a considerable influence on the strains and the displacements of the

pavement caused by the imposed horizontal displacements of the bridge. The following three modes of deformation (Figure 41) can arise:

- *Elongation of the pavement and cracking (Figure 41(a))*: The strain distribution in the pavement and the maximum value of strains can potentially cause cracking in the pavement. On the basis of measurements made during the tests, the maximum strain in the pavement ε_{pav} in the case of bridge shortening (elongation of the pavement) is approximately $\varepsilon_{pav,edg} \approx \frac{0.3 \cdot u_{imp}}{e_{TS,extr}}$, where u_{imp} is the imposed displacement at the bridge end. The factor 0.3 in this equation needs to be checked against additional experimental data. An increase of the depth $e_{TS,extr}$ is favourable as it reduces the risk of a crack in the pavement.

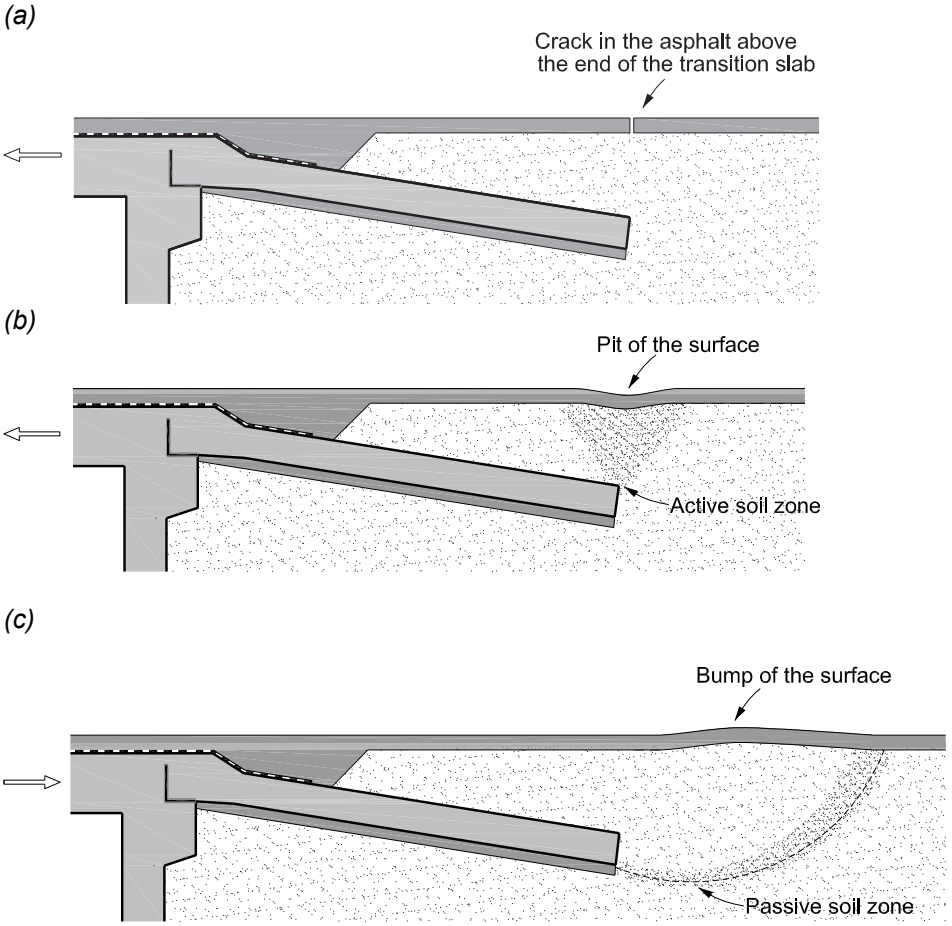

Figure 41: Potential problems on the pavement: (a) crack due to bridge shortening; (b) settlement above the end of the transition slab due to bridge shortening; (c) uplift due to bridge elongation

- Settlement in the pavement above the end of the transition slab in case of bridge shortening (Figure 41(b)): the extent of this settlement, its maximum value and the resulting curvature of the pavement, which can potentially exceed the limits recommended in the VSS code [SN 640 521c] (Figure 3), decrease sharply when the buried depts. $e_{TS,extr}$ increases, because, for a given horizontal displacement of the transition slab, the deformations in the soil are smaller (Figure 28(a) and (e) compared to (c), figure 32).

- Uplift of *the pavement in case of bridge elongation* (Figure 41(c)): the same considerations apply to this mode of deformation (Figure 30(a) and (e) compared to (c), figure 32)

Consequently, if a larger deformation capacity is needed, an increase of the buried depth $e_{TS,extr}$ is very effective. This increase can be achieved by extending the length of the transition slab, by increasing its inclination or by increasing the initial depth at the bridge end of the transition slab. As highlighted in the following recommendation, a very inclined transition slab can also have negative effects on the behaviour of the system. On the other side, the depth $e_{TS,extr}$ plays an adverse role as it increases the horizontal force in the case of bridge elongation.

c) Inclination of the transition slab

A very inclined transition slab, in combination with a smooth top surface (which is common), can cause sliding of the soil above the slab with the formation of a crack in the pavement close to the bridge end (Figure 42 (a)). This phenomenon was observed in TST3 and may be amplified by the vibrations induced by traffic loads.

In the case of a very smooth bottom surface (which is generally not the case if the transition slab is cast in situ directly on the lean concrete), the system can also slide on an inclined plane (Figure 42 (b)). In this case, if the slab is very inclined, the soil above the slab uplifts considerably when the bridge shortens, so that the discontinuity at the end of the transition slab becomes important (Figure 42 (b)). A similar but inverse discontinuity also occurs when the bridge expands (lowering of the soil above the transition slab and uplift of the soil behind the end of the slab). On the basis of the tests results, a transition slab with an inclination of 20% can already be problematic in case of a smooth top surface (common case).

(a)

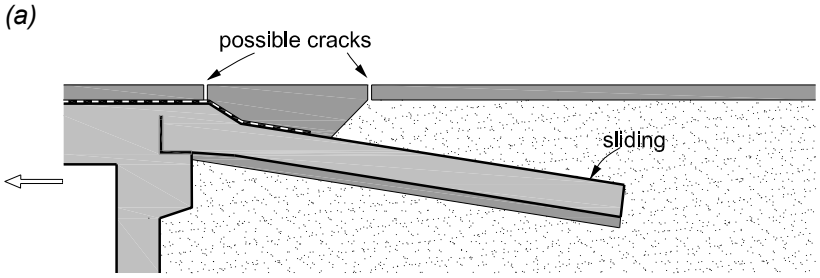

(b)

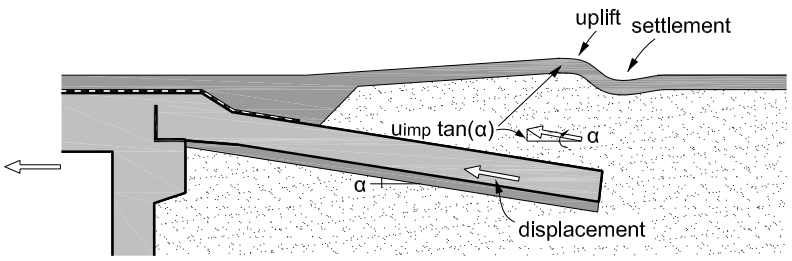

Figure 42: Potential damages due to the sliding of the transition slab on the soil in case of a smooth top surface of the transition slab: (a) crack in the pavement due to sliding of the soil above the transition slab; (b) vertical displacement of the pavement due to soil movement on an inclined plane

Another potential problem is related to the activation of large flexural moments in the transition slab due to these additional forces, for which the slab needs to be dimensioned, Figure 43. This was observed in the pushing phase of TST3, Figure 30(e).

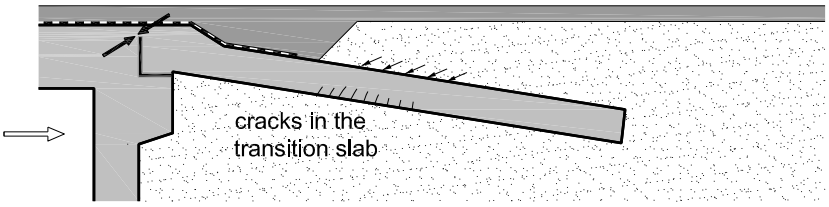

Figure 43: Bending of the transition slab in case of bridge elongation

d) Presence of a fixed wall between the bridge end and the embankment soil

As shown in Figure 44(a), the presence of a fixed back wall at the end of the abutment induces large forces in the soil beneath and in the transition slab. This strongly differentiates semi-integral bridges, which are close to this configuration, from fully integral bridges as shown in Figure 1(b), in which the abutment wall moves with the bridge, without inducing substantial forces in the ground. The choice of the type of bridge end should be made after a careful investigation of the consequences on the transition slab and the back wall.

For existing bridges in which expansion joints are to be removed, the solution of Figure 44 is the more practical solution, as there is likely to be a visiting chamber in the abutment to allow inspecting the bearings. When the bridge shortens, the passive soil pressure behind the wall increases considerably with the inclination of the transition slab. This can lead to cracking of the back wall or of the connection between the transition slab and the abutment (mainly due to the vertical component of the force that is activated, Figure 44(a)). This effect can be reduced by leaving an empty space underneath the transition slab (Figure 44(b)).The additional forces acting on the existing back wall must be taken into consideration and the back wall may need to the strengthened.

(a)

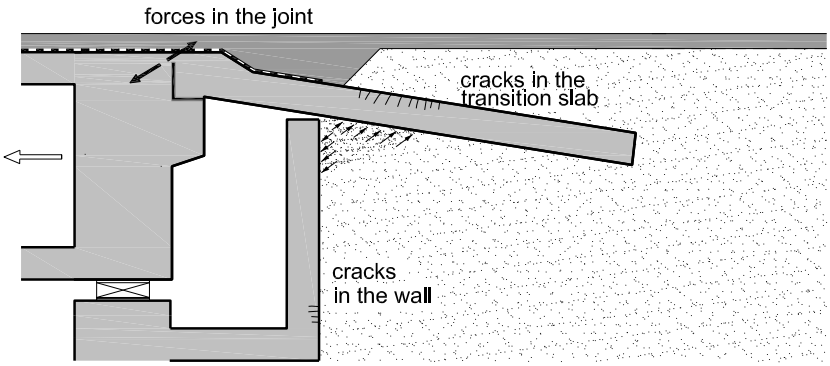

(b)

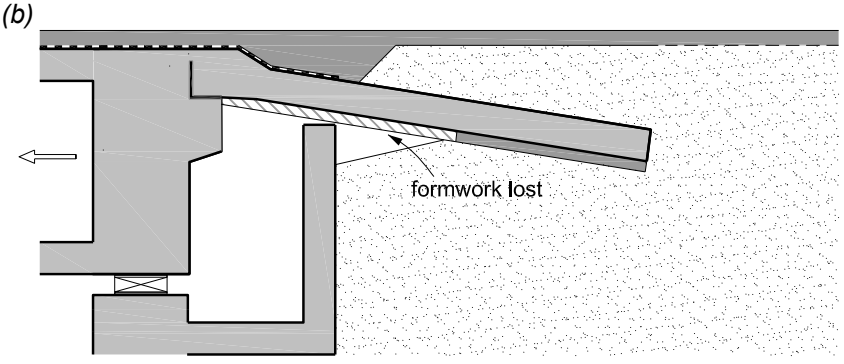

Figure 44: Potential problems for transitions slabs with a large inclination: (a) large reaction force induced by the back wall; (b) possibility of reduction of the reaction force

e) Roughness of the surfaces

The smooth surfaces of the transition slab (top surface float-finished and bottom surface smooth by the use of a PVC sheet for example) are favourable for decreasing the forces caused by the imposed displacement, but as discussed before (Figure 42), are unfavourable concerning the behaviour of the pavement. They should thus be avoided and, moreover, the top surface of the transition slab should be made rough.

f) Deformation capacity of asphalt

The experimental tests described in this report show that this parameter is fundamental to avoid cracking of the pavement. The type of the asphalt layers should be chosen to ensure a sufficient deformation capacity in case of low temperatures, as it is the most critical design situation for the asphalt layer. Pavement formulations with a high content of polymer modified bitumen should be investigated for their suitability in these critical areas.

5 Proposals for Future Research

The tests described in this report were conceived to investigate the problems that can arise when large imposed displacements from the bridge deck need to be transferred to the soil. The parameters of the tests exceed typical values for practical applications: relatively large deformation speed, very rough or very smooth surfaces of the transition slab, large variation of the inclination of the transition slab, perfectly hinged joint between the transition slab and the bridge end. Additional testing, with parameters closer to real applications could thus be useful.

Moreover, in the framework of this research, no numerical simulations were performed to interpret the results obtained. In this regard, it would be interesting to simulate the experimental results with the numerical simulation methods described in “AGB 2005/018 Ponts à culées intégrales” [DREIER 2010].

The tests confirm that the asphalt surface presents a strongly viscous behaviour. Consequently, its deformation capacity essentially depends on the deformation rate, the temperature and the type of the material used. Detailed knowledge on the behaviour of asphalt is available in the domain of the classic pavement applications (relatively large deformation speed, small strains), while for the application to transition slabs (cyclic seasonal and daily deformations, strain values up to 20 mm/m), the available knowledge is insufficient. It would be thus useful to extend investigation on the behaviour of asphalt on small scale samples, but in conditions representative of this particular application.

List of appendices

Appendix A – Reinforced concrete plans (Setup, reaction wall and back wall, transition slab)

PLAN 1 : 50

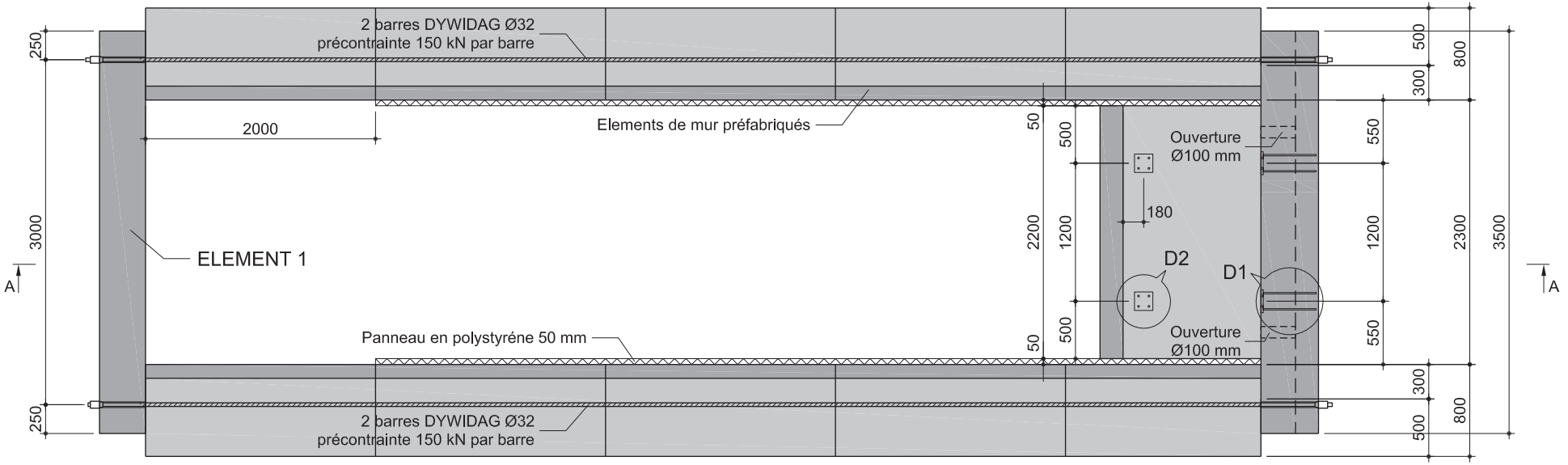

SECTION A - A 1 : 50

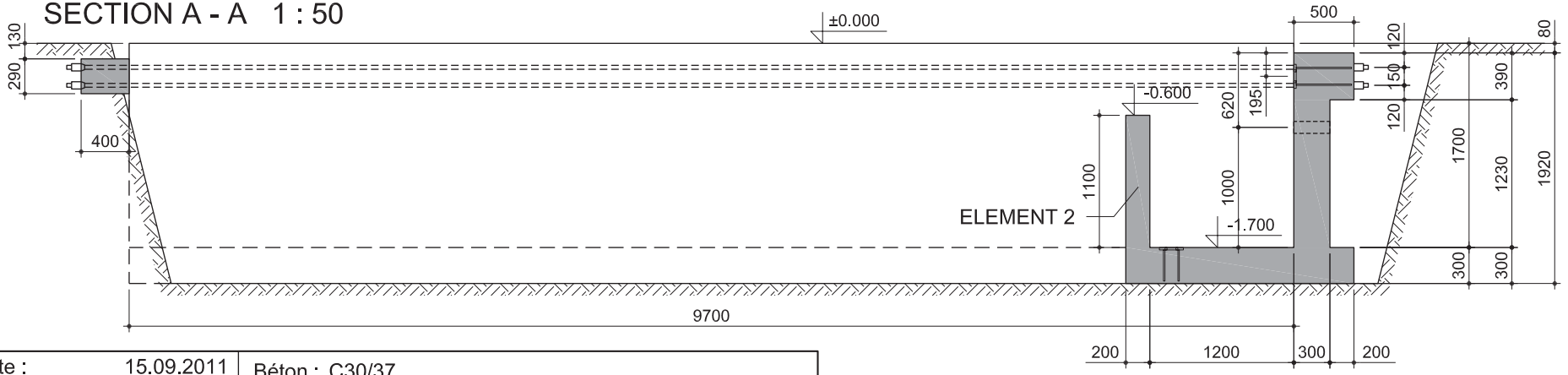

Date :	15.09.2011	Béton : C30/37
Des. : JE	Con. : -	
Révisions :		
-		
-		
-		

Pont semi-intégral

Bâti d'essai
Plan de coffrage

EPFL - ENAC - IBETON
laboratoire de construction en béton

Plan N° : 2011-11.01-101

DETAIL D1 1 : 20

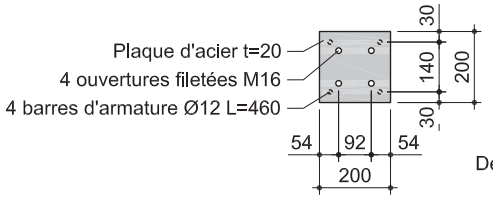

DETAIL D2 1 : 20

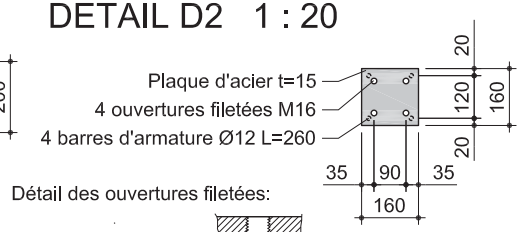

ELEMENT 1 1 : 50

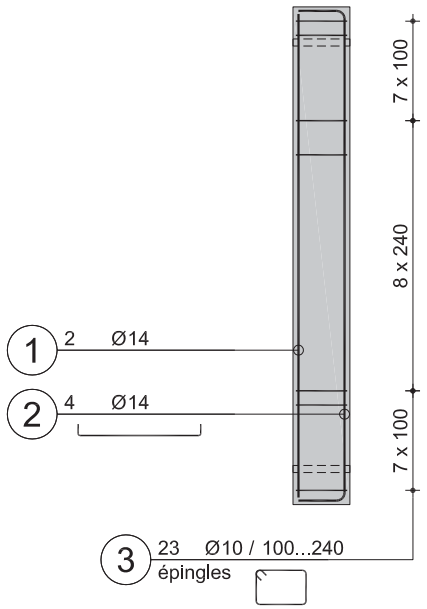

ELEMENT 2 1 : 50

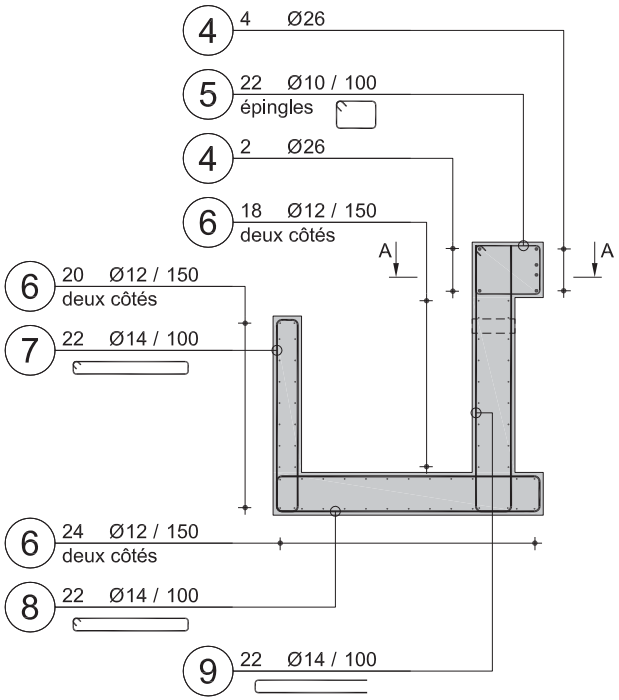

SECTION A - A 1 : 50

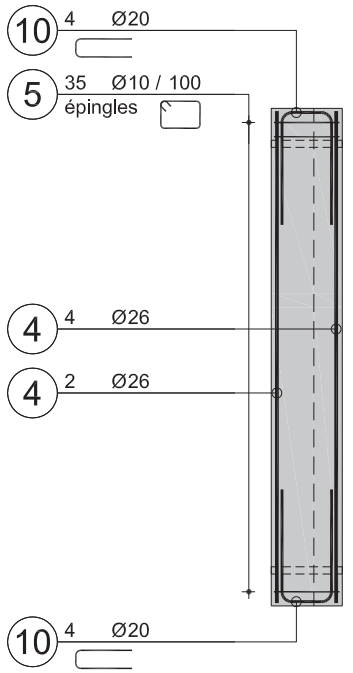

Date : 15.09.2011	Béton : C30/37
Des. : JE Con. : -	
Révisions : - - -	

Pont semi-intégral

Bâti d'essai
Plan d'armature

EPFL - ENAC - IBETON
laboratoire de construction en béton

Plan N° : 2011-11.01-102

PLAN 1 : 50
coffrage

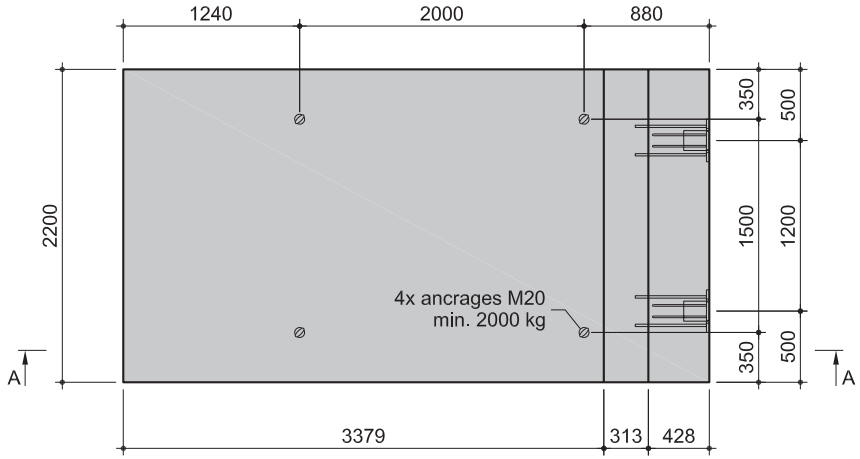

PLAN 1 : 50
armature

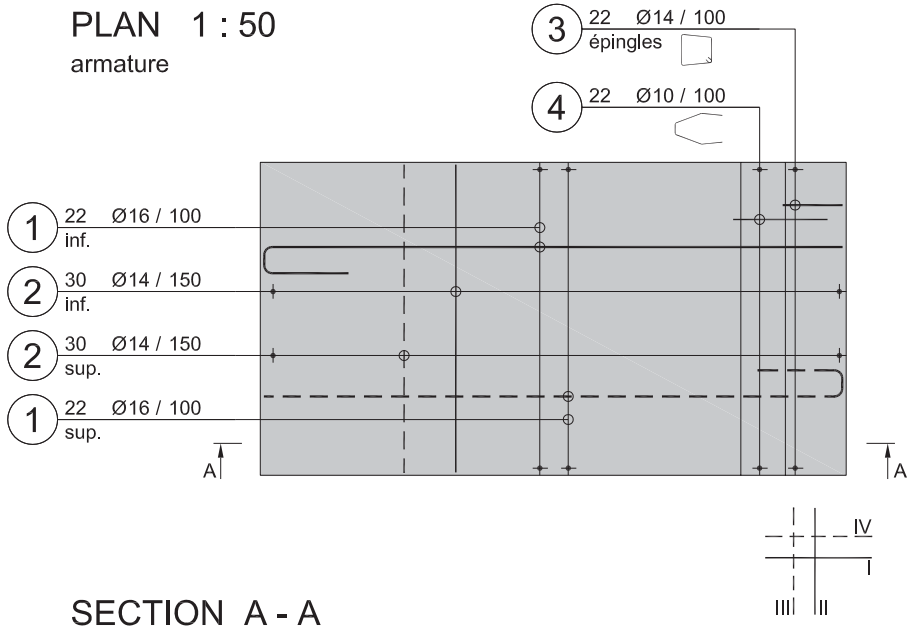

SECTION A - A

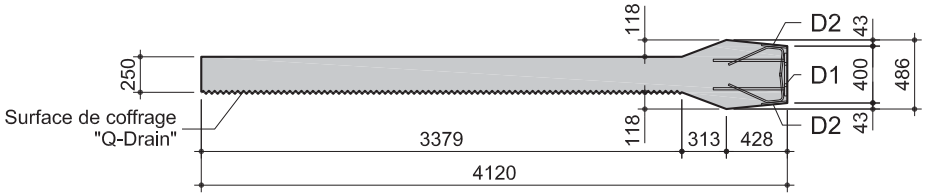

SECTION A - A

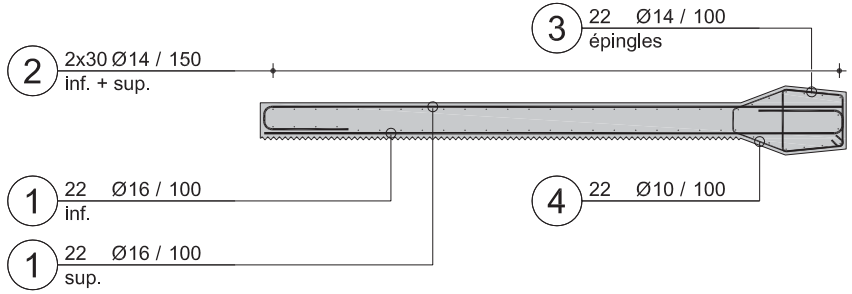

DETAIL D1 1 : 20

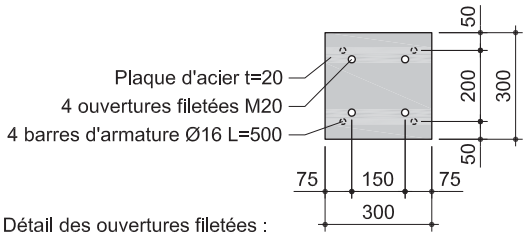

Détail des ouvertures filetées :

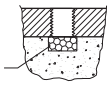

DETAIL D2 1 : 20

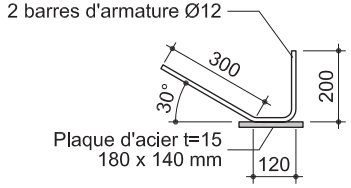

Date :	15.09.2011	Béton : C30/37
Des. : JE	Con. : -	
Révisions : - - -		

Pont semi-intégral

Dalle de transition
Plan de coffrage et d'armature

EPFL - ENAC - IBETON
laboratoire de construction en béton

Plan N° : 2011-11.01-103

Appendix B – Mechanical steel connections (Steel columns HEA160, hydraulic jacks)

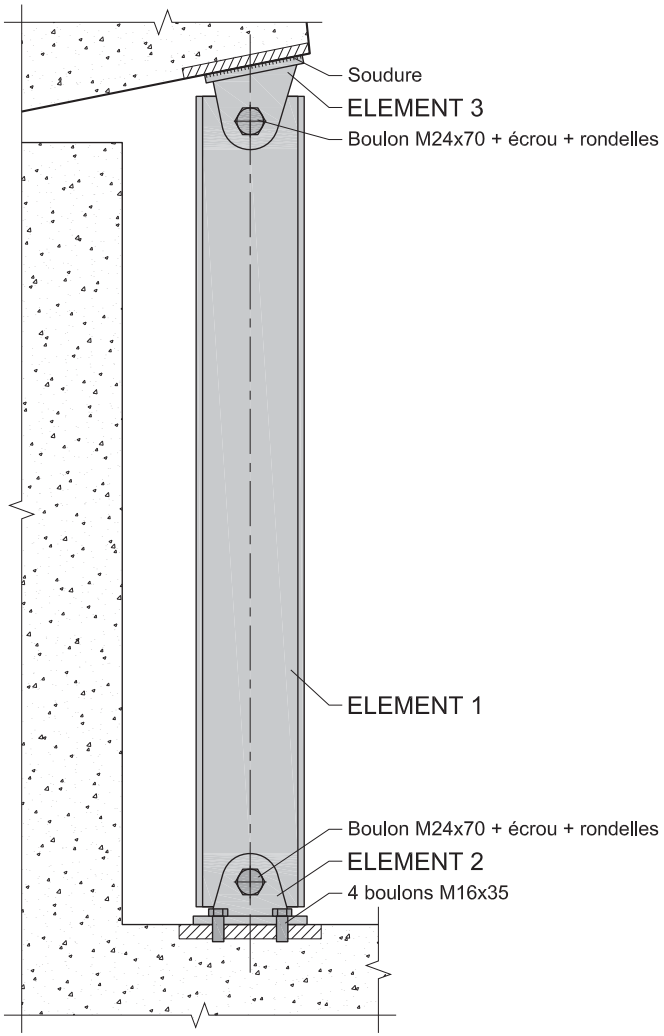

ELEMENT 1 35.7 kg 1 : 10

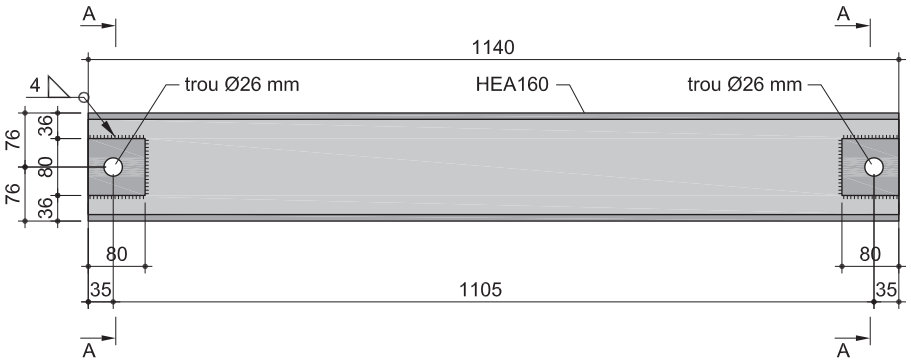

SECTION A - A

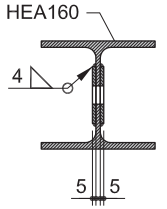

ELEMENT 2 3.0 kg

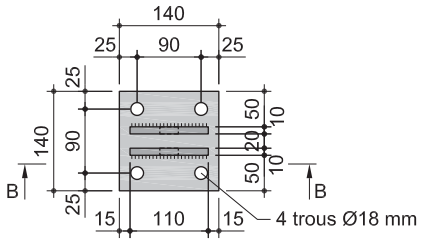

ELEMENT 3 2.8 kg

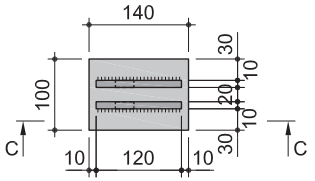

SECTION B - B

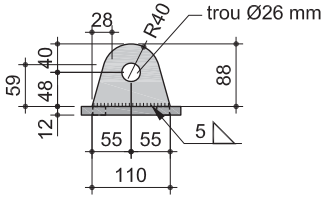

SECTION C - C

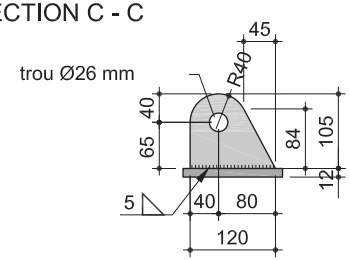

Date : 24.10.2011	Acier : S355	ELEMENT 1 - 2 pcs
Des. : JE Con. : -	Boulons : 8.8	ELEMENT 2 - 2 pcs
Révisions : - - -		ELEMENT 3 - 2 pcs

Pont semi-intégral

Bâti d'essai
Support de dalle

EPFL - ENAC - IBETON
laboratoire de construction en béton

Plan N° : 2011-11.01-201

PENTE DE DALLE 10% 1 : 10

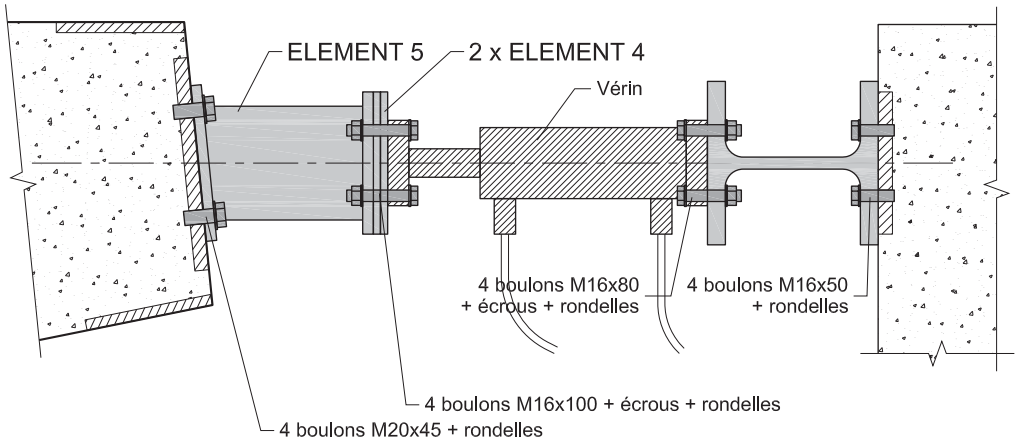

PENTE DE DALLE 20% 1 : 10

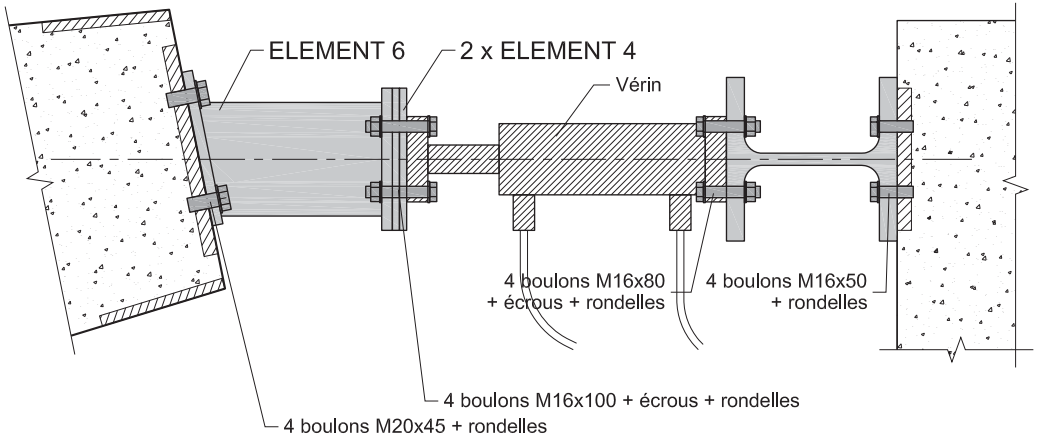

ELEMENT 4 3.1 kg

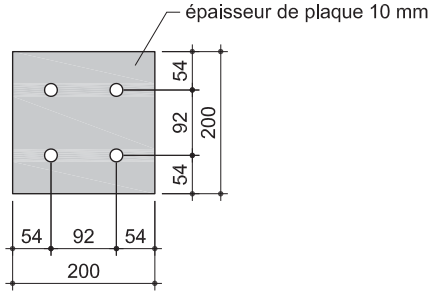

ELEMENT 5 14.5 kg

SECTION B - B

SECTION C - C

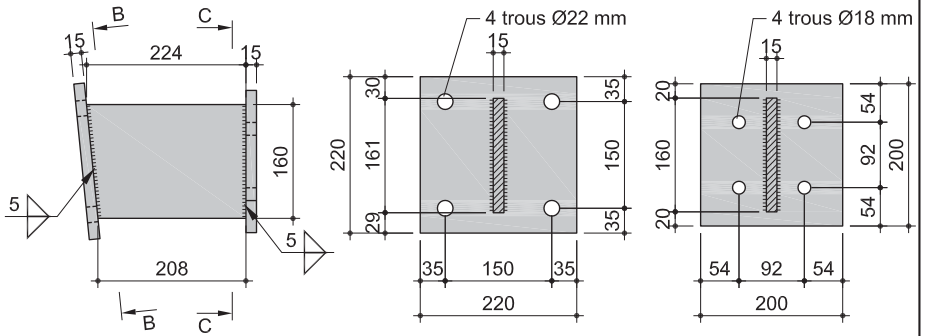

ELEMENT 6 15.0 kg

SECTION D - D

SECTION E - E

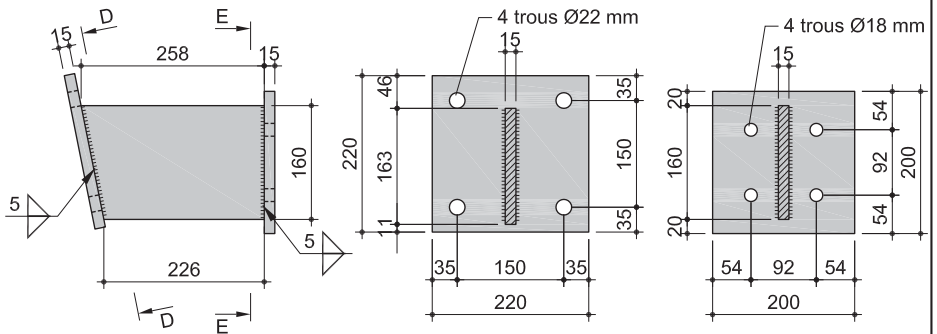

Date : 24.10.2011	Acier : S355	ELEMENT 4 - 4 pcs
Des. : JE Con. : -	Boulons : 8.8	ELEMENT 5 - 2 pcs
Révisions : - - -		ELEMENT 6 - 2 pcs

Pont semi-intégral

Bâti d'essai
Support de vérin

EPFL - ENAC - IBETON
laboratoire de construction en béton

Plan N° : 2011-11.01-202

Appendix C – Results of tachymetry for TST1 and TST2

Figure 45 and 46 show the longitudinal displacements of the pavement along axis 100 during tension and compression, measured in distance x from the bridge end.

Tension

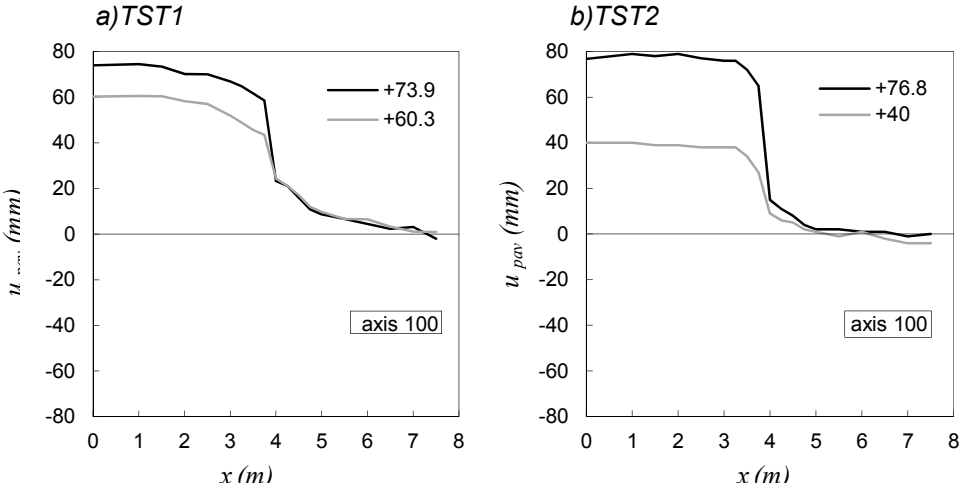

Figure 45: Longitudinal (u_{pav}) displacement of the pavement in tension- Distance from the bridge end (x)

Compression

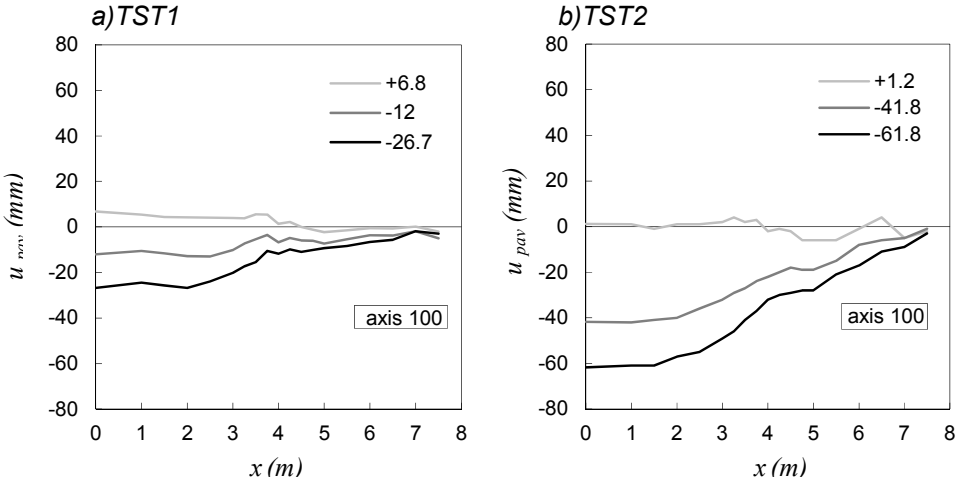

Figure 46: Longitudinal (u_{pav}) displacement of the pavement in compression- Distance from the bridge end (x)

Appendix D – Horizontal displacement of the reaction wall in TST1 and TST2

Figure 47 shows the horizontal displacement of the reaction wall as a function of the imposed force to the slab.

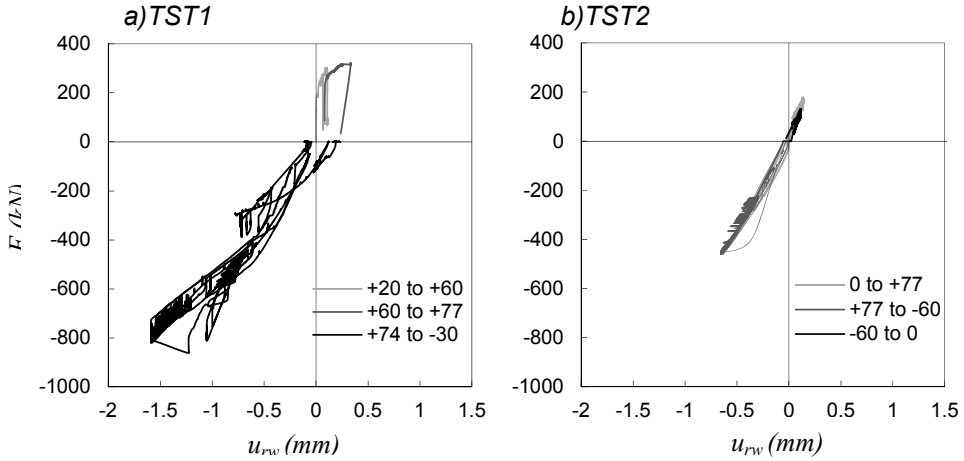

Figure 47: Force (F) - Reaction wall's horizontal displacement (u_{rw})

Appendix E – Vertical displacements of the pavement along all axes (100, 200, 300)

Tension

a)TST1

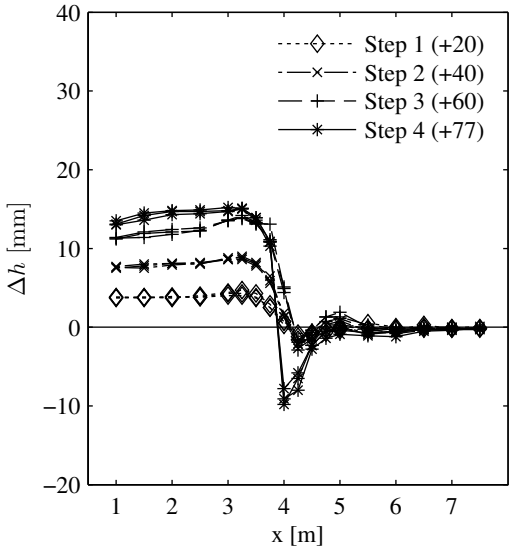

b)TST2

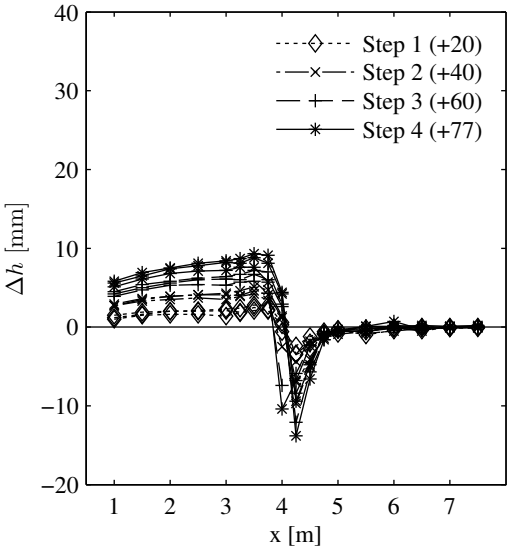

c)TST3

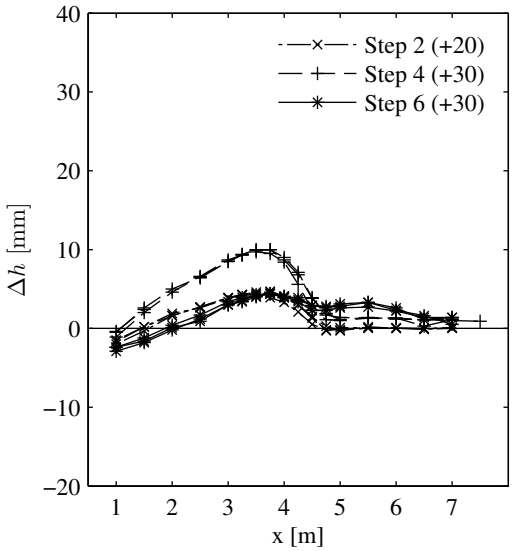

Compression

a)TST1

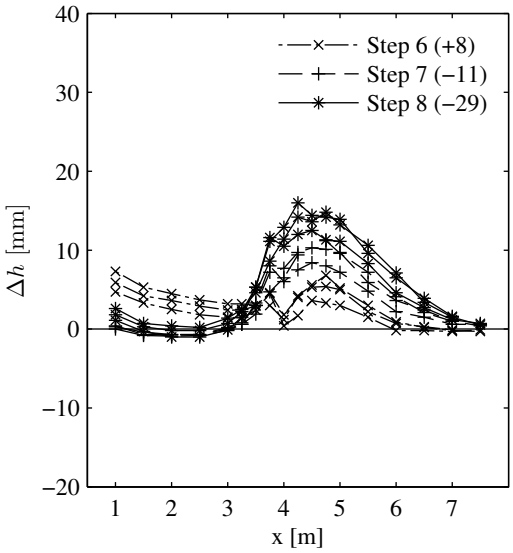

b)TST2

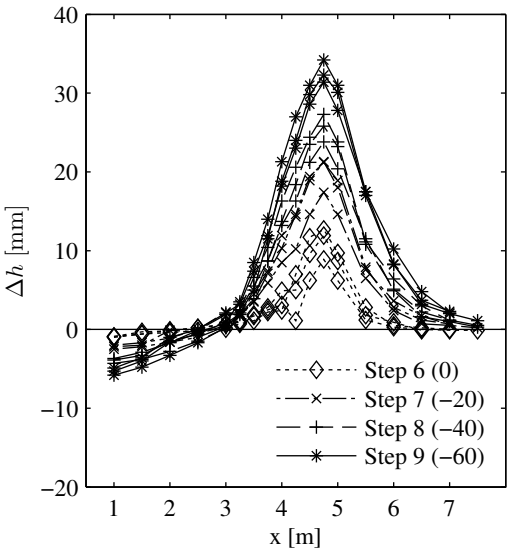

c)TST3

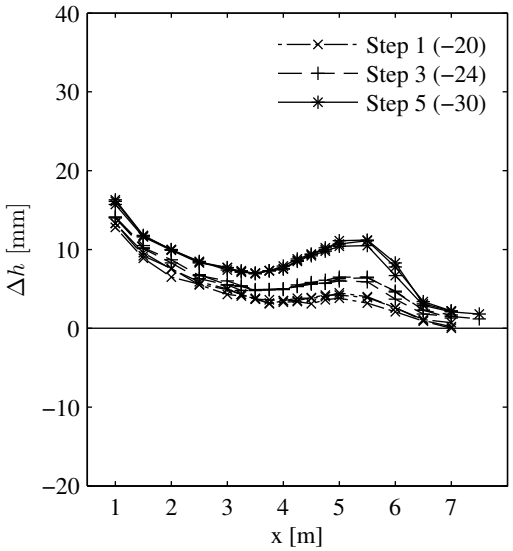

Appendix F – Displacements and applied force per test and per hour

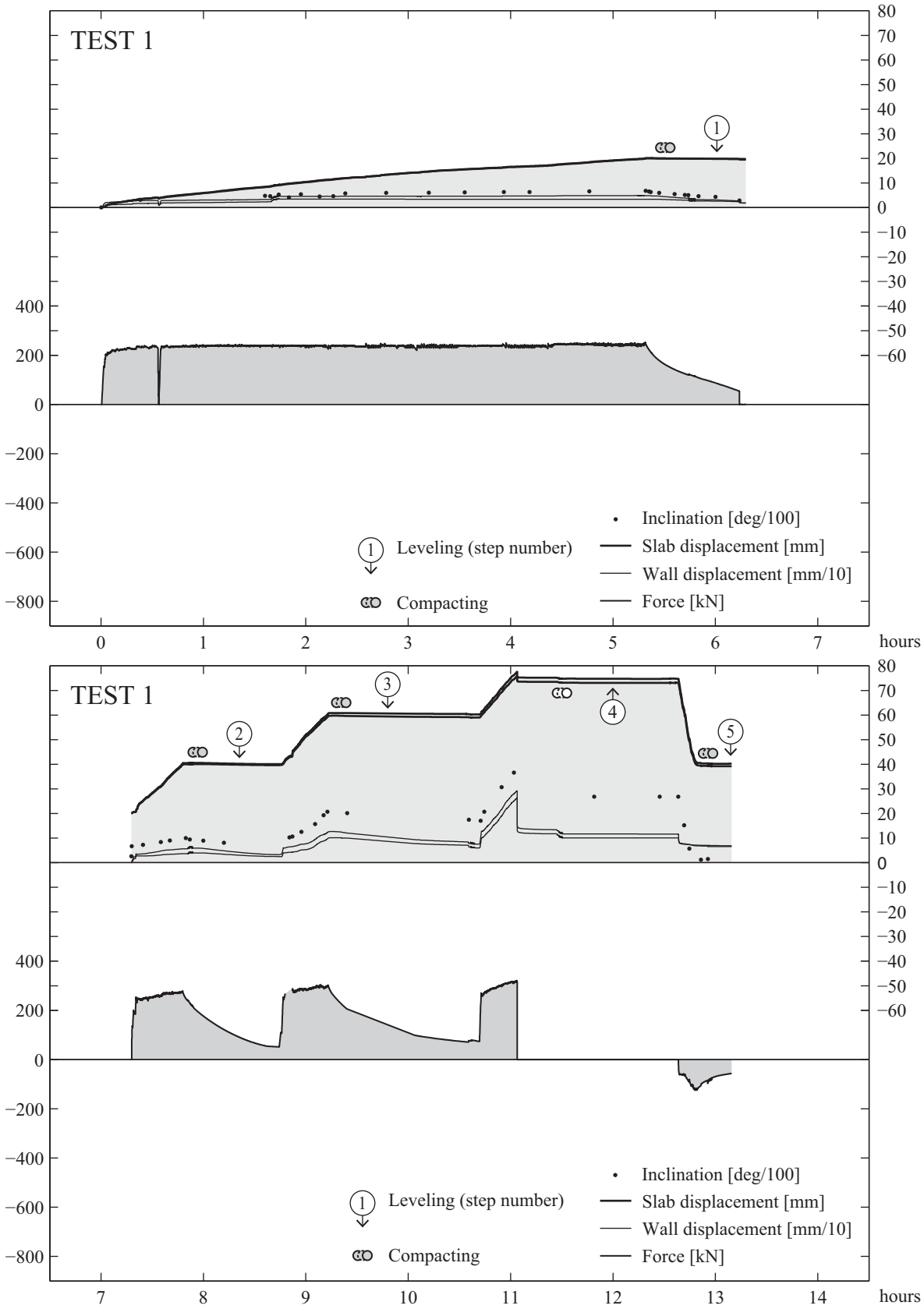

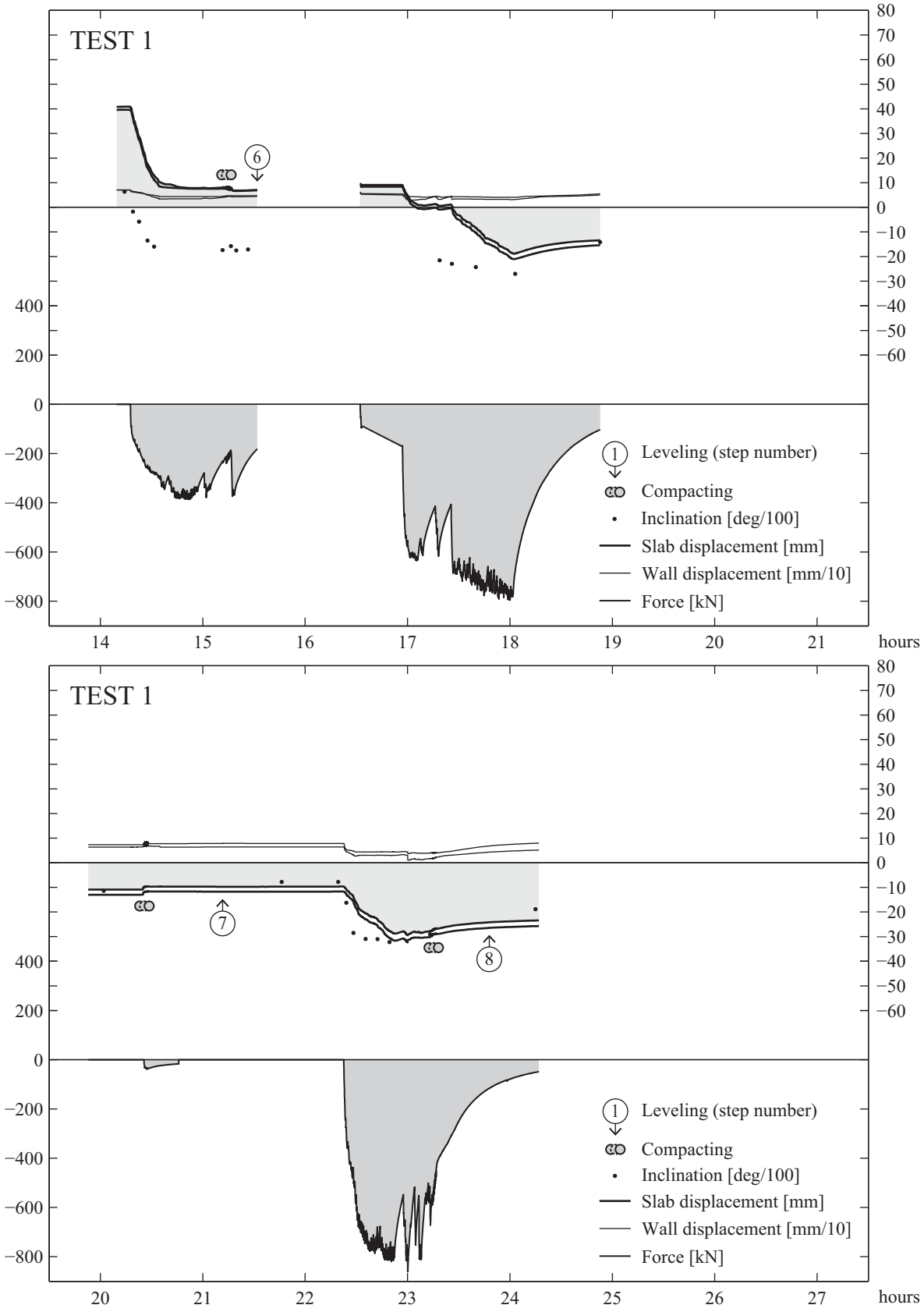
TEST 1
6
80
70
60
50
40
30
20
10
0
−10
−20
−30
−40
−50
−60
400
200
0
−200
−400
−600
−800
14
15
16
17
18
19
20
21
hours
1 Leveling (step number)
Compacting
Inclination [deg/100]
Slab displacement [mm]
Wall displacement [mm/10]
Force [kN]
TEST 1
7
8
20
21
22
23
24
25
26
27
hours

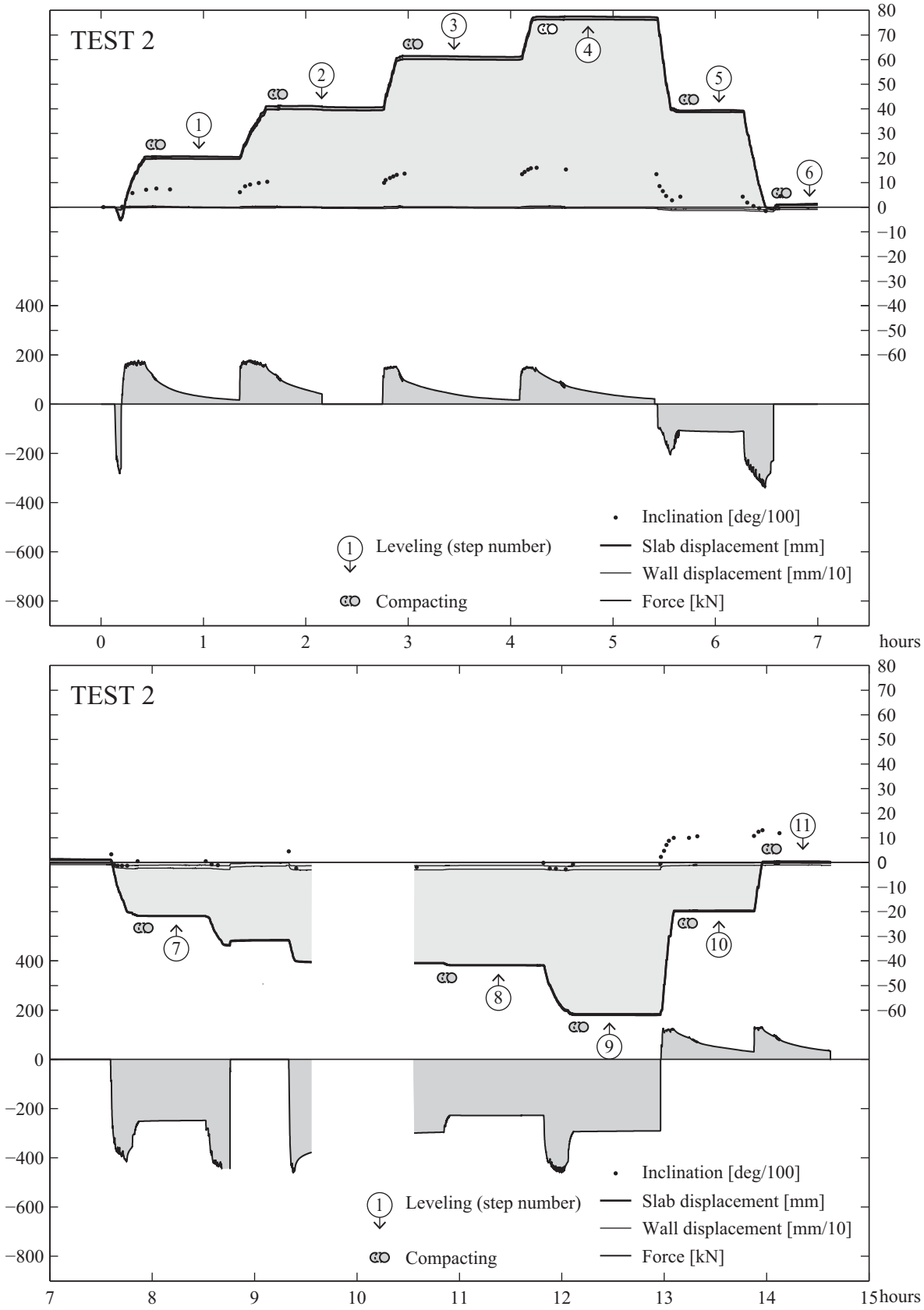
TEST 2
1
2
3
4
5
6
80
70
60
50
40
30
20
10
0
−10
−20
−30
−40
−50
−60
400
200
0
−200
−400
−600
−800
Inclination [deg/100]
Slab displacement [mm]
Wall displacement [mm/10]
Force [kN]
Leveling (step number)
Compacting
0
1
2
3
4
5
6
7
hours
TEST 2
7
8
9
10
11
7
8
9
10
11
12
13
14
15
hours

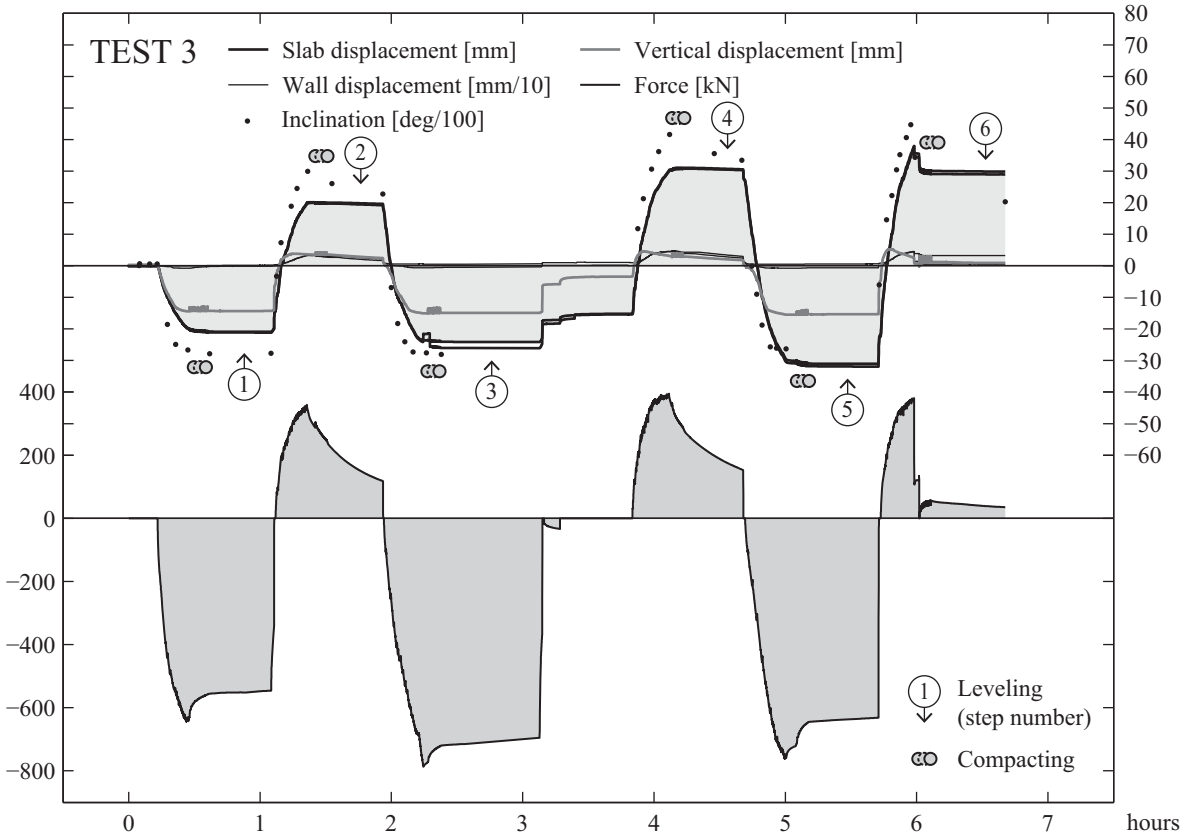
TEST 3
Slab displacement [mm]
Wall displacement [mm/10]
Inclination [deg/100]
Vertical displacement [mm]
Force [kN]
1 Leveling (step number)
Compacting
hours

Notations

Latin Letters

$e_{TS,extr}$	Buried depth of the end of the transition slab in the embankment
$e_{TS,0}$	Buried depth of the transition slab at the connection with the bridge deck
F	*Force applied to the transition slab head by the jacks*
h_{TS}	*Thickness of the transition slab*
l_{ch}	Length of the concrete hinge in the connection between the abutment and the transition slab
$L_{fp,adm}$	*Allowable distance between the fixed point and the abutment of a bridge*
L_g	*Length of the gap between the transition slab and the embankment due to settlement*
L_{TS}	*Length of the transition slab*
t	*Time (in hours or days)*
$T_{pav,be}$	*Temperature below the pavement (at the bottom of the asphalt layers)*
T_{air}	*Air temperature*
u_{imp}	*Average imposed horizontal displacement on the transition slab head*
$u_{imp,adm}$	*Maximum admissible horizontal displacement that corresponds to* χ_{adm}
$u_{TS,N}$, $u_{TS,S}$	*Horizontal displacement of the transition slab head (North or South)*
u_{pav}	*Longitudinal displacement of the pavement measured along axes 100, 200 or 300*
$u_{pav,edg}$	*Longitudinal displacement of the pavement measured at the edge (North or South)*
u_{bw}	*Average horizontal displacement of the back wall at the top*
$u_{bw,N}$, $u_{bw,S}$	*Horizontal displacement of the top of the back wall (North or South)*
u_{rw}	*Horizontal displacement of the reaction wall*
w_{crack}	*Width of crack in the pavement*
w_{pav}	*Vertical displacement of the pavement measured along axes 100, 200 or 300*
$w_{pav,max}$	*Maximum vertical displacement of the pavement at the location of the pit or bump*
w_{TS}	*Vertical displacement of the transition slab head*
x	*Distance from the bridge end*
x_{crack}	*Distance from the bridge end to the crack in the pavement*

Greek Letters

α_{TS}	*Inclination of the transition slab*
$\Delta\alpha_{TS}$	*Rotation of the transition slab head*
Δw_{pav}	*Difference of vertical displacement of the pavement in axis 100, 200 or 300*
$\varepsilon_{pav,edg}$	*Longitudinal strain of the pavement at the edge (North or South)*
ε_{imp}	*Strain of the bridge deck*
ε_{φ}	*Strain due to concrete creep*
ε_{sh}	*Strain due to shrinkage*
$\varepsilon_{\Delta T,min}$	*Strain due to maximal negative temperature variations*
$\varepsilon_{\Delta T,max}$	*Strain due to maximal positive temperature variations*
χ_{adm}	*Allowable slope variation criterion to qualify the planarity of the road pavement.*

Bibliography

[Dreier 2009], Dreier D., Muttoni A. Essais de dalles de transition, série de DT1 à DT4, Rapport d'essais, 95 p., Lausanne, December, 2009.

[Dreier 2010], Dreier D., Muttoni A. Interaction sol-structure : Ponts à culées intégrales, Rapport OFROU, N° 646, 99 p., Bern, 2010.

[Dreier 2010a], Dreier D. Modified Geometry of Transition Slabs for Integral Bridges, Proceedings of the 1st EPFL Doctoral Conference in Mechanics, Advances in Modern Aspects of Mechanics, pp. 107-110, Lausanne, February, 2010.

[Dreier 2011], Dreier D., Muttoni A., Burdet O. Transition Slabs of Integral Abutment Bridges, Structural Engineering International, Vol. 21 n° 2, pp. 144-150, May, 2011.

[Kaufmann 2005], Kaufmann W. Integrale Brücken - Sachstandsbericht, Rapport OFROU, 69 p., Bern, April, 2005.

[Kaufmann 2009], Kaufmann W. Integral Bridges: State of Practice in Switzerland, The 11th Annual International fib Symposium, Concrete: 21st century superhero, 8 p., London, UK, June, 2009.

[Kaufmann 2011], Kaufmann W., Alvarez M. Swiss Federal Roads Office Guidelines for Integral Bridges, Structural Engineering International, pp. 189-194, January, 2011.

[Kerokoski 2006], Kerokoski O. Soil-Structure Interaction of Long Jointless Bridges with Integral Abutments, Tampere University of Technology, Publication 605, 174 p., Tampere, Finland, 2006.

[Kim 2010], Kim W., Laman J. A. Integral abutment bridge response under thermal loading, Engineering structures, Elsevier Ltd, pp. 1495-1508, 2010.

[OFROU 2011], OFROU Détails de construction de ponts : directives. *CO3 : Extrémités de ponts*, Office fédéral des routes, 41 p., Bern, 2011.

[Petursson 2013], Petursson H., Kerokoski O. Monitoring and Analysis of Abutment-Soil Interaction of Two Integral Bridges, ASCE Journal of Bridge Engineering, Vol. 18, pp. 54-64, January, 2013.

[Phares 2013], Phares B., Faris A. S., Greimann L. F., Bierwagen D. Integral Bridge Abutment to Approach Slab Connection, ASCE Journal of Bridge Engineering, pp. 179-181, February, 2013.

[Pugasap 2009], Pugasap K., Kim W., Laman J. A. Long-Term Response Prediction of Integral Abutment bridges, ASCE Journal of Bridge Engineering, 14, 129-139, USA, March-April, 2009.

[SN 640 520a], SN 640 520a, Planéité : Contrôle de la géométrie, VSS, Union des professionnels suisses de la route, 8 p., Zürich, March, 1977.

[SN 640 521c], SN 640 521c, Planéité : Exigences de qualité, VSS, Association suisse des professionnels de la route et des transports, 4 p., Zürich, March, 2003.

[White 2010], White H., Petursson H., Collin P. Integral Abutment Bridges: The European Way, ASCE Practice Periodical on Structural Design and Construction, 15, pp. 201-208, USA, August, 2010.

[Zhan 2013], Zhan X., Shao X., Liu G. Thermal experiment of a Reinforced Approach Pavement for Semi- Integral Abutment Jointless Bridge, Advanced Materials Research, pp. 183-190, January, 2013.

[Zordan 2010], Zordan T., Briseghella B., Lan C. Parametric and pushover analyses on integral abutment bridge, Engineering structures, Elsevier Ltd, pp. 502-515, November, 2010.

Project closure

Schweizerische Eidgenossenschaft
Confédération suisse
Confederazione Svizzera
Confederaziun svizra

Département fédéral de l'environnement, des transports, de l'énergie et de la communication DETEC
Office fédéral des routes OFROU

RECHERCHE DANS LE DOMAINE ROUTIER DU DETEC

Formulaire N° 3 : Clôture du projet

établi / modifié le : 23 août 2013

Données de base

Projet N° :	AGB 2009/015_OBF
Titre du projet :	Vérification expérimentale des culées de ponts intégrés
Echéance effective :	Juillet 2013

Textes :

Résumé des résultats du projet :

Trois essais simulant le comportement d'une dalle de transition subissant les mouvements imposés par un pont à culée intégrée ont été effectués. Ils démontrent que ce comportement diffère notablement de celui d'une dalle de transition classique. La connexion entre le pont et la dalle de transition doit être conçue de manière à transférer des efforts de traction aussi bien que de compression. La profondeur à l'extrémité de la dalle de transition est un facteur important : plus elle est grande, moins les déformations en surface sont localisées (déf. verticales ou horizontales) ; dans ce contexte, l'inclinaison de la dalle de transition, qui est typiquement de 10 % pour beaucoup d'ouvrage, peut être choisie un peu plus forte. Par contre, d'autres phénomènes peuvent se produire lorsque l'inclinaison de la dalle de transition devient trop forte.
La différence entre un pont à culées intégrées ou semi-intégrées est notable en ce qui concerne l'amplitude des efforts dans la dalle de transition. En présence d'un mur de culée fixe (culée demi-intégrée ou transformation d'un pont classique en pont semi-intégré), les efforts dans ce mur et dans la dalle de transition sont assez élevés.
La condition de surface de la dalle de transition joue aussi un rôle : il est préférable que la dalle de transition présente une surface rugueuse à la fois sur sa face inférieure et sa face supérieure. Finalement, les déformations horizontales dans le revêtement sont très importantes, en particulier lorsque le pont se raccourcit. Il importe d'optimiser la formulation de l'enrobé utilisé pour éviter la formation prématurée de fissures dans le revêtement.

Schweizerische Eidgenossenschaft
Confédération suisse
Confederazione Svizzera
Confederaziun svizra

Département fédéral de l'environnement, des transports, de l'énergie et de la communication DETEC
Office fédéral des routes OFROU

Atteinte des objectifs :

Les buts du projet ont été atteints. Trois géométries de dalles de transition ont été essayées. Les conclusions du rapport AGB 2005/018 ont été confirmées en général. De plus, plusieurs phénomènes qui n'étaient pas couverts par l'étude théorique ont été identifiés.

Déductions et recommandations :

La connexion entre le pont et la dalle de transition doit être soigneusement étudiée.
La profondeur à l'extrémité de la dalle de transition est un paramètre important. Il est utile de l'augmenter, soit en augmentant la pente de la dalle de transition, soit en augmentant sa longueur. Il importe de ne pas aller au-delà d'environ 15% de pente.
La présence ou non d'un mur de culée fixe (pont intégré ou semi-intégré) a une forte influence sur l'amplitude des forces dans la dalle de transition.
Apartir d'une certaine inclinaison, il est souhaitable que la surface supérieure de la dalle de transition soit rendue rugueuse (comme la surface inférieure).
Pour éviter une fissuration du revêtement, il importe de développer des mélanges bitumineux permettant de plus grandes déformations spécifiques.

Publications :

en projet

Chef/cheffe de projet :

Nom : Muttoni Prénom : Aurelio

Service, entreprise, institut : Ecole Polytechnique Fédérale de Lausanne, Laboratoire de Construction en Béton (IBETON)

Signature du chef/de la cheffe de projet :

Schweizerische Eidgenossenschaft
Confédération suisse
Confederazione Svizzera
Confederaziun svizra

Département fédéral de l'environnement, des transports, de l'énergie et de la communication DETEC
Office fédéral des routes OFROU

RECHERCHE DANS LE DOMAINE ROUTIER DU DETEC

Formulaire N° 3 : Clôture du projet

Appréciation de la commission de suivi :

Evaluation :

Im Kapitel 3 der Richtlinie "konstruktive Einzelheiten von Brücken" des ASTRA werden konstruktive Lösungsvorschläge für Brückenenden integraler und semiintegraler Brücken dargelegt. Diese Angaben basieren einerseits auf der vorhandenen praktischen Erfahrung und andererseits auf dem verfügbaren nationalen und internationalen Stand der Forschung. Wie im Rahmen der theoretischen Arbeit zum Thema "Ponts à culée integrée" dargelegt wurde, kann die Gebrauchstauglichkeit von integralen Bückenenden in Abhängigkeit der Geometrie und Oberflächenbeschaffenheit der Schleppplatte beeinflusst werden. Mit dem Ziel die in dieser Arbeit gewonnenen Resultate und Aussagen zu verifizieren, wurden im Rahmen des Projekts AGB 2009/015_OBF drei grossmassstäbliche Experimente durchgeführt, bei welchen die wichtigsten geometrischen Parameter der Schleppplatte untersucht wurden. Die Experimente bestätigten die bereits auf theoretischem Weg festgestellten Einflüsse Schlepplattengeometrie auf die Boden-Bauwerks-Interaktion. Ihre Resultate bilden die Basis für die praktischen Empfehlungen für die konstruktive Ausgestaltung der Brückenenden im vorliegenden Bericht. Die im Rahmen des Projekts formulierten Zielsetzungen sind damit erreicht worden.

Mise en oeuvre :

Die dargelegten praktischen Empfehlungen im Schlussbericht geben Hinweise zur optimierten Gestaltung der Brückenenden von integralen und semiintegralen Brücken. Die Erkenntnisse können bei Umbauten oder Instandsetzungen bestehender Brücken oder bei Neubauten für die konstruktive Durchbildung der Brückenenden, insbesondere der Schlepplatten, berücksichtigt werden.

Besoin supplémentaire en matière de recherche :

Ergänzenden Forschungsbedarf im Zusammenhang mit der vorliegenden Fragestellung liegt zum einen bei weiteren Versuchen mit näher an der Wirklichkeit liegenden Parametern. In Bezug auf die monolithische Verbindung der Schleppplatte könnte bei semiintegralen Brücken auch die Trägerrotation am Brückenende von Interesse sein. Zum anderen sind die vorgeschlagenen Untersuchungen der Materialeigenschaften, insbesondere des rheologischen Verhaltens des Belags in Abhängigkeit der Temperatur und der Dehnungsgeschwindigkeit, für die Optimierung des Belags im Bereich der Schleppplatten von Bedeutung und daher forschungswürdig.

Influence sur les normes :

Die vorliegenden Erkenntnisse sollen bei der nächsten Überarbeitung des Kapitels Brückenende der Richtlinie „konstruktiven Einzelheiten von Brücken“ beachtet werden.

Président/Présidente de la commission de suivi :

Nom : Fürst Prénom : Armand

Service, entreprise, institut : Fürst Laffranchi Bauingenieure GmbH, vordere Gasse 57, 4628 Wolfwil

Signature du président/ de la présidente de la commission de suivi :

sig A. Fürst

Index of research reports on the subject of road research

L'état actuel au 31.10.2013

no. de rapport	no. de projet	titre	année
1422	ASTRA 2011/006_OBF	Fracture processes and in-situ fracture observations in Gipskeuper	2013
1421	VSS 2009/901	Experimenteller Nachweis des vorgeschlagenen Raum- und Topologiemodells für die VM-Anwendungen in der Schweiz (MDATrafo)	2013
1420	SVI 2008/003	Projektierungsfreiräume bei Strassen und Plätzen	2013
1419	VSS 2001/452	Stabilität der Polymere beim Heisseinbau von PmB-haltigen Strassenbelägen	2013
1416	FGU 2010/001	Sulfatwiderstand von Beton: verbessertes Verfahren basierend auf der Prüfung nach SIA 262/1, Anhang D	2013
1415	VSS 2010/A01	Wissenslücken im Infrastrukturmanagementprozess "Strasse" im Siedlungsgebiet	2013
1414	VSS 2010/201	Passive Sicherheit von Tragkonstruktionen der Strassenausstattung	2013
1413	SVI 2009/003	Güterverkehrsintensive Branchen und Güterverkehrsströme in der Schweiz Forschungspaket UVEK/ASTRA Strategien zum wesensgerechten Einsatz der Verkehrsmittel im Güterverkehr der Schweiz Teilprojekt B1	2013
1412	ASTRA 2010/020	Werkzeug zur aktuellen Gangliniennorm	2013
1411	VSS 2009/902	Verkehrstelematik für die Unterstützung des Verkehrsmanagements in ausserordentlichen Lagen	2013
1410	VSS 2010/202_OBF	Reduktion von Unfallfolgen bei Bränden in Strassentunneln durch Abschnittsbildung	2013
1409	ASTRA 2010/017_OBF	Regelung der Luftströmung in Strassentunneln im Brandfall	2013
1408	VSS 2000/434	Vieillissement thermique des enrobés bitumineux en laboratoire	2012
1407	ASTRA 2006/014	Fusion des indicateurs de sécurité routière : FUSAIN	2012
1406	ASTRA 2004/015	Amélioration du modèle de comportement individuell du Conducteur pour évaluer la sécurité d'un flux de trafic par simulation	2012
1405	ASTRA 2010/009	Potential von Photovoltaik an Schallschutzmassnahmen entlang der Nationalstrassen	2012
1404	VSS 2009/707	Validierung der Kosten-Nutzen-Bewertung von Fahrbahn-Erhaltungsmassnahmen	2012
1403	SVI 2007/018	Vernetzung von HLS- und HVS-Steuerungen	2012
1402	VSS 2008/403	Witterungsbeständigkeit und Durchdrückverhalten von Geokunststoffen	2012
1401	SVI 2006/003	Akzeptanz von Verkehrsmanagementmassnahmen-Vorstudie	2012
1400	VSS 2009/601	Begrünte Stützgitterböschungssysteme	2012
1399	VSS 2011/901	Erhöhung der Verkehrssicherheit durch Incentivierung	2012
1398	ASTRA 2010/019	Environmental Footprint of Heavy Vehicles Phase III: Comparison of Footprint and Heavy Vehicle Fee (LSVA) Criteria	2012
1397	FGU 2008/003_OBF	Brandschutz im Tunnel: Schutzziele und Brandbemessung Phase 1: Stand der Technik	2012
1396	VSS 1999/128	Einfluss des Umhüllungsgrades der Mineralstoffe auf die mechanischen Eigenschaften von Mischgut	2012
1395	FGU 2009/003	KarstALEA: Wegleitung zur Prognose von karstspezifischen Gefahren im Untertagbau	2012
1394	VSS 2010/102	Grundlagen Betriebskonzepte	2012
1393	VSS 2010/702	Aktualisierung SN 640 907, Kostengrundlage im Erhaltungsmanagement	2012
1392	ASTRA 2008/008_009	FEHRL Institutes WIM Initiative (Fiwi)	2012
1391	ASTRA 2011/003	Leitbild ITS-CH Landverkehr 2025/30	2012
1390	FGU 2008/004_OBF	Einfluss der Grundwasserströmung auf das Quellverhalten des Gipskeupers im Belchentunnel	2012
1389	FGU 2003/002	Long Term Behaviour of the Swiss National Road Tunnels	2012
1388	SVI 2007/022	Möglichkeiten und Grenzen von elektronischen Busspuren	2012
1387	VSS 2010/205_OBF	Ablage der Prozessdaten bei Tunnel-Prozessleitsystemen	2012
1386	VSS 2006/204	Schallreflexionen an Kunstbauten im Strassenbereich	2012
1385	VSS 2004/703	Bases pour la révision des normes sur la mesure et l'évaluation de la planéité des chaussées	2012

no. de rapport	no. de projet	titre	année
1384	VSS 1999/249	Konzeptuelle Schnittstellen zwischen der Basisdatenbank und EMF-, EMK- und EMT-DB	2012
1383	FGU 2008/005	Einfluss der Grundwasserströmung auf das Quellverhalten des Gipskeupers im Chienbergtunnel	2012
1382	VSS 2001/504	Optimierung der statischen Eindringtiefe zur Beurteilung von harten Gussasphaltsorten	2012
1381	SVI 2004/055	Nutzen von Reisezeiteinsparungen im Personenverkehr	2012
1380	ASTRA 2007/009	Wirkungsweise und Potential von kombinierter Mobilität	2012
1379	VSS 2010/206_OBF	Harmonisierung der Abläufe und Benutzeroberflächen bei Tunnel-Prozessleitsystemen	2012
1378	SVI 2004/053	Mehr Sicherheit dank Kernfahrbahnen?	2012
1377	VSS 2009/302	Verkehrssicherheitsbeurteilung bestehender Verkehrsanlagen (Road Safety Inspection)	2012
1376	ASTRA 2011/008_004	Erfahrungen im Schweizer Betonbrückenbau	2012
1375	VSS 2008/304	Dynamische Signalisierungen auf Hauptverkehrsstrassen	2012
1374	FGU 2004/003	Entwicklung eines zerstörungsfreien Prüfverfahrens für Schweissnähte von KDB	2012
1373	VSS 2008/204	Vereinheitlichung der Tunnelbeleuchtung	2012
1372	SVI 2011/001	Verkehrssicherheitsgewinne aus Erkenntnissen aus Datapooling und strukturierten Datenanalysen	2012
1371	ASTRA 2008/017	Potenzial von Fahrgemeinschaften	2011
1370	VSS 2008/404	Dauerhaftigkeit von Betonfahrbahnen aus Betongranulat	2011
1369	VSS 2003/204	Rétention et traitement des eaux de chaussée	2012
1368	FGU 2008/002	Soll sich der Mensch dem Tunnel anpassen oder der Tunnel dem Menschen?	2011
1367	VSS 2005/801	Grundlagen betreffend Projektierung, Bau und Nachhaltigkeit von Anschlussgleisen	2011
1366	VSS 2005/702	Überprüfung des Bewertungshintergrundes zur Beurteilung der Strassengriffigkeit	2010
1365	SVI 2004/014	Neue Erkenntnisse zum Mobilitätsverhalten dank Data Mining?	2011
1364	SVI 2009/004	Regulierung des Güterverkehrs Auswirkungen auf die Transportwirtschaft Forschungspaket UVEK/ASTRA Strategien zum wesensgerechten Einsatz der Verkehrsmittel im Güterverkehr der Schweiz TP D	2012
1363	VSS 2007/905	Verkehrsprognosen mit Online -Daten	2011
1362	SVI 2004/012	Aktivitätenorientierte Analyse des Neuverkehrs	2012
1361	SVI 2004/043	Innovative Ansätze der Parkraumbewirtschaftung	2012
1360	VSS 2010/203	Akustische Führung im Strassentunnel	2012
1359	SVI 2004/003	Wissens- und Technologientransfer im Verkehrsbereich	2012
1358	SVI 2004/079	Verkehrsanbindung von Freizeitanlagen	2012
1357	SVI 2007/007	Unaufmerksamkeit und Ablenkung: Was macht der Mensch am Steuer?	2012
1356	SVI 2007/014	Kooperation an Bahnhöfen und Haltestellen	2011
1355	FGU 2007/002	Prüfung des Sulfatwiderstandes von Beton nach SIA 262/1, Anhang D: Anwendbarkeit und Relevanz für die Praxis	2011
1354	VSS 2003/203	Anordnung, Gestaltung und Ausführung von Treppen, Rampen und Treppenwegen	2011
1353	VSS 2000/368	Grundlagen für den Fussverkehr	2011
1352	VSS 2008/302	Fussgängerstreifen (Grundlagen)	2011
1351	ASTRA 2009/001	Development of a best practice methodology for risk assessment in road tunnels	2011
1350	VSS 2007/904	IT-Security im Bereich Verkehrstelematik	2011
1349	VSS 2003/205	In-Situ-Abflussversuche zur Untersuchung der Entwässerung von Autobahnen	2011
1348	VSS 2008/801	Sicherheit bei Parallelführung und Zusammentreffen von Strassen mit der Schiene	2011
1347	VSS 2000/455	Leistungsfähigkeit von Parkierungsanlagen	2010
1346	ASTRA 2007/004	Quantifizierung von Leckagen in Abluftkanälen bei Strassentunneln mit konzentrierter Rauchabsaugung	2010
1345	SVI 2004/039	Einsatzbereiche verschiedener Verkehrsmittel in Agglomerationen	2011
1344	VSS 2009/709	Initialprojekt für das Forschungspaket "Nutzensteigerung für die Anwender des SIS"	2011
1343	VSS 2009/903	Basistechnologien für die intermodale Nutzungserfassung im Personenverkehr	2011
1342	FGU 2005/003	Untersuchungen zur Frostkörperbildung und Frosthebung beim Gefrierverfahren	2010
1341	FGU 2007/005	Design aids for the planning of TBM drives in squeezing ground	2011

no. de rapport	no. de projet	titre	année
1340	SVI 2004/051	Aggressionen im Verkehr	2011
1339	SVI 2005/001	Widerstandsfunktionen für Innerorts-Strassenabschnitte ausserhalb des Einflussbereiches von Knoten	2010
1338	VSS 2006/902	Wirkungsmodelle für fahrzeugseitige Einrichtungen zur Steigerung der Verkehrssicherheit	2009
1337	ASTRA 2006/015	Development of urban network travel time estimation methodology	2011
1336	ASTRA 2007/006	SPIN-ALP: Scanning the Potential of Intermodal Transport on Alpine Corridors	2010
1335	VSS 2007/502	Stripping bei lärmmindernden Deckschichten unter Überrollbeanspruchung im Labormassstab	2011
1334	ASTRA 2009/009	Was treibt uns an? Antriebe und Treibstoffe für die Mobilität von Morgen	2011
1333	SVI 2007/001	Standards für die Mobilitätsversorgung im peripheren Raum	2011
1332	VSS 2006/905	Standardisierte Verkehrsdaten für das verkehrsträgerübergreifende Verkehrsmanagement	2011
1331	VSS 2005/501	Rückrechnung im Strassenbau	2011
1330	FGU 2008/006	Energiegewinnung aus städtischen Tunneln: Systemeevaluation	2010
1329	SVI 2004/073	Alternativen zu Fussgängerstreifen in Tempo-30-Zonen	2010
1328	VSS 2005/302	Grundlagen zur Quantifizierung der Auswirkungen von Sicherheitsdefiziten	2011
1327	VSS 2006/601	Vorhersage von Frost und Nebel für Strassen	2010
1326	VSS 2006/207	Erfolgskontrolle Fahrzeugrückhaltesysteme	2011
1325	SVI 2000/557	Indices caractéristiques d'une cité-vélo. Méthode d'évaluation des politiques cyclables en 8 indices pour les petites et moyennes communes.	2010
1324	VSS 2004/702	Eigenheiten und Konsequenzen für die Erhaltung der Strassenverkehrsanlagen im überbauten Gebiet	2009
1323	VSS 2008/205	Ereignisdetektion im Strassentunnel	2011
1322	SVI 2005/007	Zeitwerte im Personenverkehr: Wahrnehmungs- und Distanzabhängigkeit	2008
1321	VSS 2008/501	Validation de l'oedomètre CRS sur des échantillons intacts	2010
1320	VSS 2007/303	Funktionale Anforderungen an Verkehrserfassungssysteme im Zusammenhang mit Lichtsignalanlagen	2010
1319	VSS 2000/467	Auswirkungen von Verkehrsberuhigungsmassnahmen auf die Lärmimmissionen	2010
1318	FGU 2006/001	Langzeitquellversuche an anhydritführenden Gesteinen	2010
1317	VSS 2000/469	Geometrisches Normalprofil für alle Fahrzeugtypen	2010
1316	VSS 2001/701	Objektorientierte Modellierung von Strasseninformationen	2010
1315	VSS 2006/904	Abstimmung zwischen individueller Verkehrsinformation und Verkehrsmanagement	2010
1314	VSS 2005/203	Datenbank für Verkehrsaufkommensraten	2008
1313	VSS 2001/201	Kosten-/Nutzenbetrachtung von Strassenentwässerungssystemen, Ökobilanzierung	2010
1312	SVI 2004/006	Der Verkehr aus Sicht der Kinder: Schulwege von Primarschulkindern in der Schweiz	2010
1311	VSS 2000/543	VIABILITE DES PROJETS ET DES INSTALLATIONS ANNEXES	2010
1310	ASTRA 2007/002	Beeinflussung der Luftströmung in Strassentunneln im Brandfall	2010
1309	VSS 2008/303	Verkehrsregelungssysteme - Modernisierung von Lichtsignalanlagen	2010
1308	VSS 2008/201	Hindernisfreier Verkehrsraum - Anforderungen aus Sicht von Menschen mit Behinderung	2010
1307	ASTRA 2006/002	Entwicklung optimaler Mischgüter und Auswahl geeigneter Bindemittel; D-A-CH - Initialprojekt	2008
1306	ASTRA 2008/002	Strassenglätte-Prognosesystem (SGPS)	2010
1305	VSS 2000/457	Verkehrserzeugung durch Parkierungsanlagen	2009
1304	VSS 2004/716	Massnahmenplanung im Erhaltungsmanagement von Fahrbahnen	2008
1303	ASTRA 2009/010	Geschwindigkeiten in Steigungen und Gefällen; Überprüfung	2010
1302	VSS 1999/131	Zusammenhang zwischen Bindemitteleigenschaften und Schadensbildern des Belages?	2010
1301	SVI 2007/006	Optimierung der Strassenverkehrsunfallstatistik durch Berücksichtigung von Daten aus dem Gesundheitswesen	2009

no. de rapport	no. de projet	titre	année
1300	VSS 2003/903	SATELROU Perspectives et applications des méthodes de navigation pour la télématique des transports routiers et pour le système d'information de la route	2010
1299	VSS 2008/502	Projet initial - Enrobés bitumineux à faibles impacts énergétiques et écologiques	2009
1298	ASTRA 2007/012	Griffigkeit auf winterlichen Fahrbahnen	2010
1297	VSS 2007/702	Einsatz von Asphaltbewehrungen (Asphalteinlagen) im Erhaltungsmanagement	2009
1296	ASTRA 2007/008	Swiss contribution to the Heavy-Duty Particle Measurement Programme (HD-PMP)	2010
1295	VSS 2005/305	Entwurfsgrundlagen für Lichtsignalanlagen und Leitfaden	2010
1294	VSS 2007/405	Wiederhol- und Vergleichspräzision der Druckfestigkeit von Gesteinskörnungen am Haufwerk	2010
1293	VSS 2005/402	Détermination de la présence et de l'efficacité de dope dans les bétons bitumineux	2010
1292	ASTRA 2006/004	Entwicklung eines Pflanzenöl-Blockheizkraftwerkes mit eigener Ölmühle	2010
1291	ASTRA 2009/005	Fahrmuster auf überlasteten Autobahnen Simultanes Berechnungsmodell für das Fahrverhalten auf Autobahnen als Grundlage für die Berechnung von Schadstoffemissionen und Fahrzeitgewinnen	2010
1290	VSS 1999/209	Conception et aménagement de passages inférieurs et supérieurs pour piétons et deux-roues légers	2008
1289	VSS 2005/505	Affinität von Gesteinskörnungen und Bitumen, nationale Umsetzung der EN	2010
1288	ASTRA 2006/020	Footprint II - Long Term Pavement Performance and Environmental Monitoring on A1	2010
1287	VSS 2008/301	Verkehrsqualität und Leistungsfähigkeit von komplexen ungesteuerten Knoten: Analytisches Schätzverfahren	2009
1286	VSS 2000/338	Verkehrsqualität und Leistungsfähigkeit auf Strassen ohne Richtungstrennung	2010
1285	VSS 2002/202	In-situ Messung der akustischen Leistungsfähigkeit von Schallschirmen	2009
1284	VSS 2004/203	Evacuation des eaux de chaussée par les bas-cotés	2010
1283	VSS 2000/339	Grundlagen für eine differenzierte Bemessung von Verkehrsanlagen	2008
1282	VSS 2004/715	Massnahmenplanung im Erhaltungsmanagement von Fahrbahnen: Zusatzkosten infolge Vor- und Aufschub von Erhaltungsmassnahmen	2010
1281	SVI 2004/002	Systematische Wirkungsanalysen von kleinen und mittleren Verkehrsvorhaben	2009
1280	ASTRA 2004/016	Auswirkungen von fahrzeuginternen Informationssystemen auf das Fahrverhalten und die Verkehrssicherheit Verkehrspsychologischer Teilbericht	2010
1279	VSS 2005/301	Leistungsfähigkeit zweistreifiger Kreisel	2009
1278	ASTRA 2004/016	Auswirkungen von fahrzeuginternen Informationssystemen auf das Fahrverhalten und die Verkehrssicherheit - Verkehrstechnischer Teilbericht	2009
1277	SVI 2007/005	Multimodale Verkehrsqualitätsstufen für den Strassenverkehr - Vorstudie	2010
1276	VSS 2006/201	Überprüfung der schweizerischen Ganglinien	2008
1275	ASTRA 2006/016	Dynamic Urban Origin - Destination Matrix - Estimation Methodology	2009
1274	SVI 2004/088	Einsatz von Simulationswerkzeugen in der Güterverkehrs- und Transportplanung	2009
1273	ASTRA 2008/006	UNTERHALT 2000 - Massnahme M17, FORSCHUNG: Dauerhafte Materialien und Verfahren SYNTHESE - BERICHT zum Gesamtprojekt "Dauerhafte Beläge" mit den Einzelnen Forschungsprojekten: - ASTRA 200/419: Verhaltensbilanz der Beläge auf Nationalstrassen - ASTRA 2000/420: Dauerhafte Komponenten auf der Basis erfolgreicher Strecken - ASTRA 2000/421: Durabilité des enrobés - ASTRA 2000/422: Dauerhafte Beläge, Rundlaufversuch - ASTRA 2000/423: Griffigkeit der Beläge auf Autobahnen, Vergleich zwischen den Messergebnissen von SRM und SCRIM - ASTRA 2008/005: Vergleichsstrecken mit unterschiedlichen oberen Tragschichten auf einer Nationalstrasse	2008
1272	VSS 2007/304	Verkehrsregelungssysteme - behinderte und ältere Menschen an Lichtsignalanlagen	2010
1271	VSS 2004/201	Unterhalt von Lärmschirmen	2009

no. de rapport	no. de projet	titre	année
1270	VSS 2005/502	Interaktion Strasse Hangstabilität: Monitoring und Rückwärtsrechnung	2009
1269	VSS 2005/201	Evaluation von Fahrzeugrückhaltesystemen im Mittelstreifen von Autobahnen	2009
1268	ASTRA 2005/007	PM10-Emissionsfaktoren von Abriebspartikeln des Strassenverkehrs (APART)	2009
1267	VSS 2007/902	MDAinSVT Einsatz modellbasierter Datentransfernormen (INTERLIS) in der Strassenverkehrstelematik	2009
1266	VSS 2000/343	Unfall- und Unfallkostenraten im Strassenverkehr	2009
1265	VSS 2005/701	Zusammenhang zwischen dielektrischen Eigenschaften und Zustandsmerkmalen von bitumenhaltigen Fahrbahnbelägen (Pilotuntersuchung)	2009
1264	SVI 2004/004	Verkehrspolitische Entscheidfindung in der Verkehrsplanung	2009
1263	VSS 2001/503	Phénomène du dégel des sols gélifs dans les infrastructures des voies de communication et les pergélisols alpins	2006
1262	VSS 2003/503	Lärmverhalten von Deckschichten im Vergleich zu Gussasphalt mit strukturierter Oberfläche	2009
1261	ASTRA 2004/018	Pilotstudie zur Evaluation einer mobilen Grossversuchsanlage für beschleunigte Verkehrslastsimulation auf Strassenbelägen	2009
1260	FGU 2005/001	Testeinsatz der Methodik "Indirekte Vorauserkundung von wasserführenden Zonen mittels Temperaturdaten anhand der Messdaten des Lötschberg-Basistunnels	2009
1259	VSS 2004/710	Massnahmenplanung im Erhaltungsmanagement von Fahrbahnen - Synthesebericht	2008
1258	VSS 2005/802	Kaphaltestellen Anforderungen und Auswirkungen	2009
1257	SVI 2004/057	Wie Strassenraumbilder den Verkehr beeinflussen Der Durchfahrtswiderstand als Arbeitsinstrument bei der städtebaulichen Gestaltung von Strassenräumen	2009
1256	VSS 2006/903	Qualitätsanforderungen an die digitale Videobild-Bearbeitung zur Verkehrsüberwachung	2009
1255	VSS 2006/901	Neue Methoden zur Erkennung und Durchsetzung der zulässigen Höchstgeschwindigkeit	2009
1254	VSS 2006/502	Drains verticaux préfabriqués thermiques pour la consolidation in-situ des sols	2009
1253	VSS 2001/203	Rétention des polluants des eaux de chausées selon le système "infilitrations sur les talus". Vérification in situ et optimisation	2009
1252	SVI 2003/001	Nettoverkehr von verkehrsintensiven Einrichtungen (VE)	2009
1251	ASTRA 2002/405	Incidence des granulats arrondis ou partiellement arrondis sur les propriétés d'ahérence des bétons bitumineux	2008
1250	VSS 2005/202	Strassenabwasser Filterschacht	2007
1249	FGU 2003/004	Einflussfaktoren auf den Brandwiderstand von Betonkonstruktionen	2009
1248	VSS 2000/433	Dynamische Eindringtiefe zur Beurteilung von Gussasphalt	2008
1247	VSS 2000/348	Anforderungen an die strassenseitige Ausrüstung bei der Umwidmung von Standstreifen	2009
1246	VSS 2004/713	Massnahmenplanung im Erhaltungsmanagement von Fahrbahnen: Bedeutung Oberflächenzustand und Tragfähigkeit sowie gegenseitige Beziehung für Gebrauchs- und Substanzwert	2009
1245	VSS 2004/701	Verfahren zur Bestimmung des Erhaltungsbedarfs in kommunalen Strassennetzen	2009
1244	VSS 2004/714	Massnahmenplanung im Erhaltungsmanagement von Fahrbahnen - Gesamtnutzen und Nutzen-Kosten-Verhältnis von standardisierten Erhaltungsmassnahmen	2008
1243	VSS 2000/463	Kosten des betrieblichen Unterhalts von Strassenanlagen	2008
1242	VSS 2005/451	Recycling von Ausbauasphalt in Heissmischgut	2007
1241	ASTRA 2001/052	Erhöhung der Aussagekraft des LCPC Spurbildungstests	2009
1240	ASTRA 2002/010	L'acceptabilité du péage de congestion : Résultats et analyse de l'enquête en Suisse	2009
1239	VSS 2000/450	Bemessungsgrundlagen für das Bewehren mit Geokunststoffen	2009
1238	VSS 2005/303	Verkehrssicherheit an Tagesbaustellen und bei Anschlüssen im Baustellenbereich von Hochleistungsstrassen	2008
1237	VSS 2007/903	Grundlagen für eCall in der Schweiz	2009

no. de rapport	no. de projet	titre	année
1236	ASTRA 2008/008_07	Analytische Gegenüberstellung der Strategie- und Tätigkeitsschwerpunkte ASTRA-AIPCR	2008
1235	VSS 2004/711	Forschungspaket Massnahmenplanung im EM von Fahrbahnen - Standardisierte Erhaltungsmassnahmen	2008
1234	VSS 2006/504	Expérimentation in situ du nouveau drainomètre européen	2008
1233	ASTRA 2000/420	Unterhalt 2000 Forschungsprojekt FP2 Dauerhafte Komponenten bitumenhaltiger Belagsschichten	2009
651	AGB 2006/006_OBF	Instandsetzung und Monitoring von AAR-geschädigten Stützmauern und Brücken	2013
650	AGB 2005/010	Korrosionsbeständigkeit von nichtrostenden Betonstählen	2012
649	AGB 2008/012	Anforderungen an den Karbonatisierungswiderstand von Betonen	2012
648	AGB 2005/023 + AGB 2006/003	Validierung der AAR-Prüfungen für Neubau und Instandsetzung	2011
647	AGB 2004/010	Quality Control and Monitoring of electrically isolated post- tensioning tendons in bridges	2011
646	AGB 2005/018	Interactin sol-structure : ponts à culées intégrales	2010
645	AGB 2005/021	Grundlagen für die Verwendung von Recyclingbeton aus Betongranulat	2010
644	AGB 2005/004	Hochleistungsfähiger Faserfeinkornbeton zur Effizienzsteigerung bei der Erhaltung von Kunstbauten aus Stahlbeton	2010
643	AGB 2005/014	Akustische Überwachung einer stark geschädigten Spannbetonbrücke und Zustandserfassung beim Abbruch	2010
642	AGB 2002/006	Verbund von Spanngliedern	2009
641	AGB 2007/007	Empfehlungen zur Qualitätskontrolle von Beton mit Luftpermeabilitätsmessungen	2009
640	AGB 2003/011	Nouvelle méthode de vérification des ponts mixtes à âme pleine	2010
639	AGB 2008/003	RiskNow-Falling Rocks Excel-basiertes Werkzeug zur Risikoermittlung bei Steinschlagschutzgalerien	2010
638	AGB2003/003	Ursachen der Rissbildung in Stahlbetonbauwerken aus Hochleistungsbeton und neue Wege zu deren Vermeidung	2008
637	AGB 2005/009	Détermination de la présence de chlorures à l'aide du Géoradar	2009
636	AGB 2002/028	Dimensionnement et vérification des dalles de roulement de ponts routiers	2009
635	AGB 2004/002	Applicabilité de l'enrobé drainant sur les ouvrages d'art du réseau des routes nationales	2008
634	AGB 2002/007	Untersuchungen zur Potenzialfeldmessung an Stahlbetonbauten	2008
633	AGB 2002/014	Oberflächenschutzsysteme für Betontragwerke	2008
632	AGB 2008/201	Sicherheit des Verkehrssystem Strasse und dessen Kunstbauten Testregion - Methoden zur Risikobeurteilung Schlussbericht	2010
631	AGB 2000/555	Applications structurales du Béton Fibré à Ultra-hautes Performances aux ponts	2008
630	AGB 2002/016	Korrosionsinhibitoren für die Instandsetzung chloridverseuchter Stahlbetonbauten	2010
629	AGB 2003/001 + AGB 2005/019	Integrale Brücken - Sachstandsbericht	2008
628	AGB 2005/026	Massnahmen gegen chlorid-induzierte Korrosion und zur Erhöhung der Dauerhaftigkeit	2008
627	AGB 2002/002	Eigenschaften von normalbreiten und überbreiten Fahrbahnübergängen aus Polymerbitumen nach starker Verkehrsbelastung	2008
626	AGB 2005/110	Sicherheit des Verkehrssystems Strasse und dessen Kunstbauten: Baustellensicherheit bei Kunstbauten	2009
625	AGB 2005/109	Sicherheit des Verkehrssystems Strasse und dessen Kunstbauten: Effektivität und Effizienz von Massnahmen bei Kunstbauten	2009
624	AGB 2005/108	Sicherheit des Verkehrssystems / Strasse und dessen Kunstbauten / Risikobeurteilung für Kunstbauten	2010
623	AGB 2005/107	Sicherheit des Verkehrssystems Strasse und dessen Kunstbauten: Tragsicherheit der bestehenden Kunstbauten	2009
622	AGB 2005/106	Rechtliche Aspekte eines risiko- und effizienzbasierten Sicherheitskonzepts	2009
621	AGB 2005/105	Sicherheit des Verkehrssystems Strasse und dessen Kunstbauten Szenarien der Gefahrenentwicklung	2009

no. de rapport	no. de projet	titre	année
620	AGB 2005/104	Sicherheit des Verkehrssystems Strasse und dessen Kunstbauten: Effektivität und Effizienz von Massnahmen	2009
619	AGB 2005/103	Sicherheit des Verkehrssystems / Strasse und dessen Kunstbauten / Ermittlung des Netzrisikos	2010
618	AGB 2005/102	Sicherheit des Verkehrssystems Strasse und dessen Kunstbauten: Methodik zur vergleichenden Risikobeurteilung	2009
617	AGB 2005/100	Sicherheit des Verkehrssystems Strasse und dessen Kunstbauten Synthesebericht	2010
616	AGB 2002/020	Beurteilung von Risiken und Kriterien zur Festlegung akzeptierter Risiken in Folge aussergewöhnlicher Einwirkungen bei Kunstbauten	2009